The molecular ecology of *Microcystis* sp. blooms in the San Francisco Estuary

Timothy G. Otten,[1,2]* Hans W. Paerl,[2]
Theo W. Dreher,[1] Wim J. Kimmerer[3] and
Alexander E. Parker[3,4]

[1]*Department of Microbiology, Oregon State University, 226 Nash Hall, Corvallis, OR, 97331, USA.*

[2]*Institute of Marine Sciences, University of North Carolina at Chapel Hill, 3431 Arendell St, Morehead City, NC, 28557, USA.*

[3]*Romburg Tiburon Center, San Francisco State University, 3150 Paradise Dr, Tiburon, CA, 94920, USA.*

[4]*California State University Maritime Academy, 200 Maritime Academy Drive, Vallejo, CA, 94590, USA.*

Summary

Harmful blooms of the cyanobacterium *Microcystis* sp. have become increasingly pervasive in the San Francisco Estuary Delta (USA) since the early 2000s and their rise has coincided with substantial decreases in several important fish species. Direct and indirect effects *Microcystis* blooms may have on the Delta food web were investigated. The *Microcystis* population was tracked for 2 years at six sites throughout the Delta using quantitative PCR. High-throughput amplicon sequencing and colony PCR sequencing revealed the presence of 10 different strains of *Microcystis*, including 6 different microcystin-producing strains. Shotgun metagenomic analysis identified a variety of *Microcystis* secondary metabolite pathways, including those for the biosynthesis of: aeruginosin, cyanopeptolin, microginin, microviridin and piriclamide. A sizable reduction was observed in microbial community diversity during a large *Microcystis* bloom ($H = 0.61$) relative to periods preceding ($H = 2.32$) or following ($H = 3.71$) the bloom. Physicochemical conditions of the water column were stable throughout the bloom period. The elevated abundance of a cyanomyophage with high similarity to previously sequenced isolates known to infect *Microcystis* sp. was implicated in the

bloom's collapse. Network analysis was employed to elucidate synergistic and antagonistic relationships between *Microcystis* and other bacteria and indicated that only very few taxa were positively correlated with *Microcystis*.

Introduction

Cyanobacterial blooms dominated by potentially toxic *Microcystis* sp. have become more frequent throughout the San Francisco Estuary (SFE) Delta since the early 2000s (Lehman *et al.*, 2013). Concomitantly, populations of four pelagic fishes have been in decline throughout the SFE Delta since 2002; a phenomenon referred to as the pelagic organism decline (POD) (Sommer *et al.*, 2007; Thomson *et al.*, 2010). The temporal and spatial overlap of these two trends raises the possibility that *Microcystis* blooms have contributed to the declining fish populations (Acuña *et al.*, 2012). The SFE is the largest estuary on the U.S. Pacific coast and consists of five major zones spanning the marine–freshwater continuum.

Secondary metabolites produced by cyanobacterial blooms may directly impair fish health and fitness (Wiegand and Pflugmacher, 2005; Leflaive and Ten-Hage, 2007). The hepatotoxin microcystin can cause histopathological effects in the organs of fish and can impair juvenile development (Malbrouck and Kestemont, 2006). Microcystins have been identified in the liver tissue of delta smelt (*Hypomesmus transpacificus*) harvested from the Delta, with liver necrosis and lesions characteristic of microcystin exposure also observed in long lived POD-impacted species including the striped bass, *Morone saxatilis* (Lehman *et al.*, 2010). *Microcystis* blooms may also indirectly influence POD fishes by altering food web structure through competition (Smith, 1986; Huisman *et al.*, 2004) or by releasing allelopathic compounds (Smith and Doan, 1999; Legrand *et al.*, 2003; Sedmak and Eleršek, 2005) that inhibit the growth of other, more nutritious phytoplankton (e.g., diatoms and cryptophytes) (Ferrão-Filho *et al.*, 2000; Von Elert and Wolffrom, 2001; Von Elert *et al.*, 2003). Calanoid copepods are the main prey of most SFE fish larvae and juvenile delta smelt (Hobbs *et al.*, 2006; Slater and Baxter, 2014). Laboratory feeding studies have demonstrated that *Microcystis* sp. is a poor food source for the

predominant calanoid copepods in the Delta, *Eurytemora affinis* and *Pseudodiaptomus forbesi* (Ger *et al.*, 2010), likely due to the large size of colonies (Burnsd and Hegarty, 1994), their lack of sterols and fatty acids (Lampert, 1987) and their production of toxic secondary metabolites (Wilson *et al.*, 2006).

Long-term monitoring data provide insights into how the Delta aquatic food web has changed over the past several decades in response to increasing demands for irrigation and drinking water, climate change, and a series of aquatic species invasions. In addition to the putative effects of cyanobacterial blooms, a number of other stressors are believed to negatively influence POD species, including: increased salinity (Feyrer *et al.*, 2007), decreased total suspended solids (Nobriga *et al.*, 2005), increased water temperatures (Komoroske *et al.*, 2014), extensive water pumping and fish entrainment (Kimmerer, 2005; Sommer *et al.*, 2007), anthropogenic contaminants (e.g., heavy metals and pesticides) (Brooks *et al.*, 2012), excessive nutrient loading (Jassby, 2008), invasive aquatic vegetation (Hestir, 2010) and introductions of the invasive overbite clam (*Potamocorbula amurensis*) and Asian clam (*Corbicula fluminea*) (Nichols *et al.*, 1990; Alpine and Cloern, 1992). Combined, these stressors have resulted in decreased food availability and quality throughout the food web (Sommer *et al.*, 2007; Hammock *et al.*, 2015).

While there has been considerable research conducted on phytoplankton–cyanobacterial interactions, few studies have investigated how cyanobacterial blooms affect non-photoautotrophic bacteria in the water column (Bagatini *et al.*, 2014; Woodhouse *et al.*, 2016). Conversely, associated bacteria (and viruses) may directly or indirectly influence the fitness of cyanobacterial blooms (e.g., cell lysis, nutrient cycling, vitamin synthesis, etc.) (Cole, 1982). Due to competitive exclusion, cyanobacterial blooms tend to reduce the abundance of other, more nutritious primary producers (Paerl and Otten, 2013). Under such conditions, the microbial loop, which relies upon abundant heterotrophic bacteria and bacterivorous microzooplankton, becomes more important in sustaining macrozooplankton populations during cyanobacterial bloom events (Christoffersen *et al.*, 1990; Moustaka-Gouni and Vardaka, 2006; Krevš *et al.*, 2010). Therefore, heterotrophic bacteria comprise an important linkage in the microbial food web as they recycle a large percentage of carbon fixed by primary producing photoautotrophs through the microbial loop (Søndergaard *et al.*, 1985). Pelagic food webs are influenced by bottom-up and top-down factors; as lakes increase in trophic status, the percent contribution of plankton biomass (as μg C L^{-1}) often skew toward cyanobacterial and protozoan dominance, whereas systems with lower trophic levels are often dominated by heterotrophic bacteria and flagellates (Auer *et al.*, 2004). During periods of low primary productivity bacterial populations are constrained by nutrient availability, whereas under high productivity conditions their populations are more constrained by protozoan grazing (Auer *et al.*, 2004). In the SFE Delta, aside from infrequent algal blooms, phytoplankton biomass remains generally low (Lucas and Thompson, 2012). Therefore, microplankton (e.g., ciliates and flagellates) grazing upon bacteria (Azam *et al.*, 1983; Porter *et al.*, 1985) likely play an essential role in transferring carbon, nutrients, fatty acids and sterols to higher trophic levels (Klein Breteler *et al.*, 1999; Bec *et al.*, 2006). Different groups of bacteria are expected to be better adapted to rapidly respond to ephemeral phytoplankton blooms and to more efficiently sequester and recycle photosynthates. *Sphingomonas*, *Flavobacterium*, *Pseudomonas*, *Nocardia* and *Paenibacillus* have all been isolated from cyanobacterial blooms and shown to degrade complex, organic compounds (Berg *et al.*, 2009), including in some cases cyanotoxins (cf. Jones *et al.*, 1994; Park *et al.*, 2001; Amé *et al.*, 2006). Likewise, members of the phylum Verrucomicrobia are ubiquitous in aquatic environments and contain representatives able to efficiently degrade polysaccharides (Martinez-Garcia *et al.*, 2012). This study is the first to characterize the microbial community within the SFE Delta and to assess how bacterial populations change in response to a cyanobacterial bloom. Although protozoan bacterivory was not assessed, it is likely that trophic upgrading by microplankton such as ciliates and flagellates (Segovia *et al.*, 2015) represents an important, linkage in the SFE food web worthy of further study. For example, previous feeding experiments using several different Delta mesozooplankters (cladocerans, cyclopoid copepods and calanoid copepods) have demonstrated that protozoan microplankton are grazed at rates at least as high as those on phytoplankton (Bouley and Kimmerer, 2006; Gifford *et al.*, 2007; York *et al.*, 2014).

Here we report the results from a 2-year study conducted in the Delta to investigate the ecology and physiology of *Microcystis* sp. blooms with an emphasis on how blooms may influence the base of the food web. We hypothesized that: (1) there would be multiple *Microcystis* strains (defined as operational taxonomic units or OTUs) widely distributed throughout the Delta due to tidal mixing and pumping; (2) the *Microcystis* sp. population would be able to produce a variety of known (e.g., microcystins) and novel secondary metabolites that could directly or indirectly degrade food web structure; and (3) *Microcystis* blooms would influence microbial community richness and structure.

Experimental procedures

Sample collection

Six surveys were conducted between July–September in 2011, a wet year, and July–October in 2012, a drought year, at six Delta sites ($n = 72$): Mildred Island (37°59′13″N, 121°31′25″W), Franks Tract (38°2′39″N, 121°36′22″W), Mokelumne River (38°7′50″N, 121°34′22″W), Old River

(37°58′51″N, 121°34′30″W), the San Joaquin River at Antioch (38°1′7″N, 121°48′27″W) and the Sacramento River at Rio Vista (38°9′13″N, 121°41′12″W). These locations were selected to include pairs of sites from similar habitats, only one of each pair having a history of producing dense *Microcystis* blooms (Supporting Information Fig. S1), to allow comparison of habitat conditions that support or repress blooms. *Microcystis* blooms often occur within flooded islands formed by levee breaches, a habitat represented by Mildred Island (breached in 1983) and Franks Tract (breached in 1937). The other study sites represent conditions in either tributary rivers in the Delta (Mokelumne River and Old River) or the main rivers (Antioch and Rio Vista). Discrete water samples were collected at 0.2 and 3 m depth at all sites, although only data from 0.2 m depth samples are presented. Temperature, pH, dissolved oxygen and salinity were measured with a Sea-Bird 19 CTD, and discrete analyses of nutrients (PO_4^-, NO_3^-, NH_4^+, urea), dissolved inorganic carbon (DIC) and chlorophyll *a* were conducted in the laboratory following standard methods (Parker *et al.*, 2012).

DNA analyses

Samples were sterile filtered onsite onto Supor membrane filters (47 mm dia. × 0.2 µm pore size) for genetic analysis and stored frozen (−80°C) until further processing. DNA was extracted from filters using GeneRite RWOC1 DNA extraction kits. Real-time quantitative PCR (QPCR) employing Taqman chemistry was performed on an ABI 7500 Fast thermal cycler (Applied Biosystems) on 1:10 diluted DNA extracted from all samples ($n = 72$) and was used to estimate the proportion of toxigenic *Microcystis* (those containing the microcystin synthase E gene; designated *mcyE*) relative to total *Microcystis* (based on c-phycocyanin pigment gene; designated *cpcA*) using standard curves derived from serially diluted plasmid constructs as previously described (Kurmayer and Kutzenberger, 2003; Otten *et al.*, 2012; Supporting Information Table S1). The average amplification efficiency of the *cpcA* assay was 99.4% (slope = −3.336, y-int. = 37.050) and that of the *mcyE* assay was 100.5% (slope = −3.311, y-int. = 37.248). The limit of quantitation for the assays was 100 copies/ml. In order to assess the diversity of *Microcystis* strains through time and space, DNA from 40 samples was individually PCR amplified in triplicate 25 µl reactions using custom 454-indexed primers containing cyanobacteria-specific 16S-23S rRNA internal transcribed spacer (ITSc) primers (Janse *et al.*, 2003; Supporting Information Table S1) and High Fidelity Accuprime Taq DNA polymerase (Invitrogen). The amplicons from each set of triplicate reactions were pooled and purified using an AMPure magnetic bead PCR cleanup kit (Agencourt). The pooled amplicons were one-way pyrosequenced (23S side) on a Roche 454 GS Junior instrument with an emPCR(Lib-L) kit at the Centre for Genome Research and Biocomputing at Oregon State University (Corvallis, OR, USA). Reads were trimmed to 324 nt and those with phred scores > 25 were clustered into operational taxonomic units (OTUs) as described below. All 454 reads were deposited into NCBI GenBank under BioSample accession number SAMN05978453.

Additionally, during one transect each year, individual *Microcystis* colonies were isolated by serial dilution under an inverted microscope, with emphasis on isolating multiple colonies of each of several unique morphologies. Individual colony isolates were resuspended in 25 µl sterile dH$_2$O, then subjected to three freeze–thaw cycles and 30 s of vortexing to lyse the cells. PCR assays targeting cyanobacteria-specific 16S-23S rRNA ITS and microcystin synthetase B (*mcyB*) genes were performed and sequenced as previously described (Otten and Paerl, 2011) (Supporting Information Table S1). Amplicon sequences were deposited into NCBI GenBank under accession numbers KY086337–KY086375. Based on the metagenome assemblies, PCR primers were also developed to detect *Microcystis* genes involved in the biosynthesis of the secondary metabolites: aeruginosin, cyanopeptolin, micropeptin, microviridin and piriclamide (*aerB*, *cpnC*, *mpnC*, *mvdB*, *pirA*, respectively), and these assays were run against DNA extracted from a *Microcytis aeruginosa* strain (UTEX 2386) used in a previous feeding study of SFE Delta copepods (Ger *et al.*, 2010).

The QPCR data indicated that the largest accumulation of *Microcystis* over the study period occurred at Mildred Island in August 2012. In an effort to elucidate potential synergistic and antagonistic relationships between Delta bacteria and *Microcystis* sp., all six samples collected at Mildred Island in 2012 were amplified using the Earth Microbiome Project's universal 16S v4 rRNA bacterial primers (515F/806R) and their recommended cycling conditions (Caporaso *et al.*, 2012; Supporting Information Table S1). As before, the reactions were carried out in triplicate reactions, then they were pooled and purified; however, instead of 454 pyrosequencing, the amplicons were sequenced on an Illumina MiSeq instrument using v3 chemistry (300 bp, paired-ends) at the OSU CGRB. Prior to amplification, the primers were modified to contain overhanging Illumina adaptor sequences (Forward: 5′-TCGTCGGCAGCGTCAGATGTGTATAAGAGACAG-[515F primer]-3′; Reverse: 5′-GTCTCGTGGGCTCGGAGATGTGTATAAGAGACAG-[806R primer]-3′) for multiplex indexing. The initial PCR consisted of 20 amplification cycles. The PCR products were purified as before and then Illumina index primers were ligated via an additional 8 cycles of amplification. Amplicons were clustered into OTUs as described below. The samples generated 109 976 raw sequencing reads, with 46 193 retained after QA/QC. All 16S rRNA reads were deposited into NCBI SRA under accession # SAMN05969162-SAMN05969167.

Shotgun metagenomics was performed on three samples (23-Jul, 27-Aug, 10-Sep) from the 2012 Mildred Island time-series corresponding to before, during and after a *Microcystis* bloom, hereafter designated as pre-, peak- and post-bloom samples. DNA libraries were created using a Nextera XT prep kit and sequenced (101 bp, paired-end reads) on an Illumina HiSeq 2000 instrument at the OSU CGRB. Reads were quality screened (phred score > 30, minimum length > 50 nucleotides) and trimmed using Trimmomatic (Bolger *et al.*, 2014). Following QA/QC processing, 142 732 275 shotgun sequencing reads were assembled into 595 647 unscaffolded contiguous sequences (contigs; max length = 219 221 nts, min length = 200 nts, mean length = 734 nts) using IDBA-UD (Peng *et al.*, 2012). To estimate community structure, individual reads were converted to amino acids using RAPSearch (Ye *et al.*, 2011) and the taxonomy of a normalized subset (∼ 1 million per sample) of protein encoding reads was classified to the lowest common ancestor using MEGAN v5 (Huson

et al., 2011). A normalized subset of reads ($\sim$ 34.6 million per sample) were mapped to the assembled contigs using BWA (Li and Durbin, 2009) and the coverage depth for each contig per sample was calculated as the average number of sequencing reads recruiting to each contig; this was done using samtools (Li *et al.*, 2009). Contigs were functionally and taxonomically characterized as previously described (Otten *et al.*, 2016). The annotated contigs and their relative read coverage depths were visualized in R using the mmgenome package (Albertsen *et al.*, 2013). Metagenome completeness (fraction of microbiome represented in a metagenomic data set) per sequencing effort was estimated from Nonpareil curves (Rodriguez-R and Konstantinidis, 2014). Additionally, the assemblies were screened bioinformatically for cyanobacterial toxin genes using a combination of BLAST and antiSMASH 2.0, to identify all known and putative nonribosomal peptide synthetase and polyketide synthases (Blin *et al.*, 2013). Contig annotation was also performed by the Joint Genome Institute, IMG Project 101107, and all raw sequencing reads were deposited into the Short Read Archive at NCBI (SAMN05880410-SAMN05880412).

Statistical and bioinformatic analyses

The general structure of microcystin is cyclo(D-Ala-L-**X**-D-MeAsp-L-**Z**-Adda-D-Glu-Mdha-, where X and Z are variable L amino acids (Tillett *et al.*, 2000). Microcystin structural variants (congeners) were predicted from the adenylation domain binding pocket signatures (Stachelhaus codes; Stachelhaus *et al.*, 1999) responsible for amino acid incorporation into the X (encoded by McyB1) and Z (encoded by McyC1) positions of the microcystin molecule (Mikalsen *et al.*, 2003). Colony PCR amplicons and contigs assembled from the shotgun metagenomes were analysed using NPRSpredictor2 (Röttig *et al.*, 2011). The 16S-23S rRNA ITS sequences acquired from the 454 pyrosequencing were grouped into operational taxonomic units (OTUs) delineated at the 97% nucleotide identity level using a *de novo* clustering approach in QIIME (usearch) as previously described (Otten *et al.*, 2015). Singleton OTUs were removed. The 454 OTUs were aligned with the Sanger sequencing results of the colony PCR amplified 16S-23S rRNA ITS and their phylogeny was inferred using a Bayesian framework implemented in MrBayes v.3.1.2 with a general time reversible substitution model with gamma distributed variation. The 16S rRNA sequences acquired from the MiSeq amplicon run were clustered into OTUs using a 97% nucleotide identity cutoff with a subsampled open-reference clustering approach in Qiime as previously described (Rideout *et al.*, 2014). Singletons were also removed from this dataset, then the bacterial community composition of each sample was compared using non-metric multidimensional scaling (NMDS) analysis using the 'vegan', 'MASS' and 'Cairo' packages in R. Microbial network co-occurrence patterns were determined based on covariance in 16S rRNA OTU rank abundances using the 'vegan', 'reshape', and 'igraph' packages in R as previously described (Williams *et al.*, 2014). Only those relationships exhibiting significant ($p < 0.05$) and strongly positive ($r > 0.75$) or negative ($r < -0.75$) Spearman's rank correlation coefficients were retained since higher correlation cutoffs are more likely to minimize random (i.e., false) pairwise interactions (Williams *et al.*, 2014).

Results

Microcystis abundance and diversity

QPCR was used to estimate total (*cpcA*-possessing) and toxigenic (*mcyE*-possessing) *Microcystis* from all samples ($n = 72$). The Rio Vista and Mokelumne River sites had the lowest total *Microcystis*, with *cpcA* maximum concentrations over the study period of only 660 and 940 copies ml^{-1} respectively. Since the phycocyanin (*cpcA*) and microcystin (*mcyE*) genes are present in single copies within the *Microcystis* chromosome, gene copies ml^{-1} approximately represent cell equivalents ml^{-1}. Moderate-to-high *Microcystis* concentrations occurred at times at the other sites with maximum cell equivalent concentrations of 15 950 cell eq ml^{-1} at Antioch, 102 160 cell eq ml^{-1} at Franks Tract, 2 430 290 cell eq ml^{-1} at Mildred Island and 105 390 cell eq ml^{-1} at Old River. The average percentage ($\pm$SD) of toxigenic *Microcystis* cell equivalents at these sites was 46% ($\pm$24), 23% ($\pm$29), 18% ($\pm$22) and 31% ($\pm$22) respectively (Fig. 1).

There were 40 435 16S-23S rRNA ITS reads retained from 40 discrete samples from the six sites. The results indicated that the cyanobacterial community was dominated by *Aphanizomenon* sp. at all sampling stations in 2011, when it comprised $\sim$ 96% of all reads, with *Microcystis* sp. representing only $\sim$ 4% of the community (Supporting Information Table S2). In contrast, *Microcystis* sp. was the most abundant cyanobacterium in 2012, when it comprised $\sim$ 53% of the cyanobacterial community, followed by *Aphanizomenon* (25%) and *Dolichospermum* (formerly *Anabaena*) at 21%. Cluster analysis suggested there were eight *Microcystis* operational taxonomic units (OTUs). In the context of this study, we consider OTUs to be synonymous with individual strains. OTUs 1 and 2 were the most abundant and comprised 38% and 36% of the total respectively. There was no evidence for any site-specific, endemic *Microcystis* populations since all eight of the delineated OTUs were at times observed in each location (Fig. 2).

Even though there were eight *Microcystis* OTUs identified by 454 pyrosequencing, only three colony morphologies were observed. Throughout the study period, *Microcystis* colonies exhibited atypical morphologies compared with colonies from other systems, with unusually large colonies (up to 1 cm dia.) presenting as either flat flakes or dense webs of cells (Supporting Information Fig. S2). In order to assess if the cells comprising each unique colony morphology were genetically distinct from the other morphologies, 20 colonies were PCR amplified and sequenced in each of 2011 and 2012. Approximately one-third of the colonies contained more than one ITS sequence, suggesting that these atypically large colonies were composed of multiple strains. Clustering and phylogenetic analysis of the ITS genes
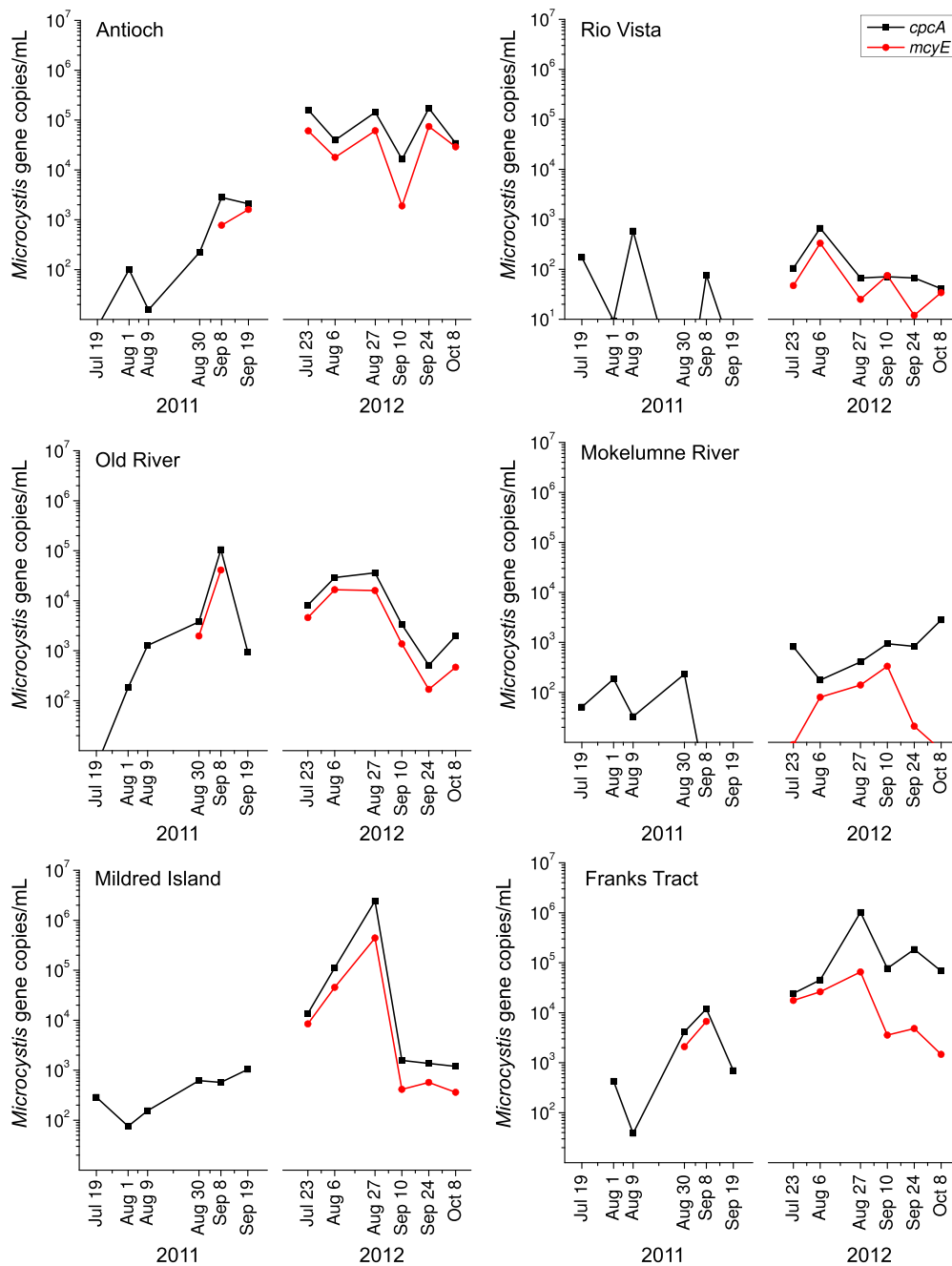
Fig. 1. QPCR estimates of total (*cpcA*) and toxigenic (*mcyE*) *Microcystis* during the summer (2011–2012) at six sampling stations throughout the SF Delta. [Colour figure can be viewed at wileyonlinelibrary.com]

revealed that colony morphologies were inconsistent with specific OTUs as there were six distinct *Microcystis* sp. clades identified from the three morphologies (Supporting Information Fig. S3); four of which were also observed in the 454 pyrosequences. Combined the two approaches identified 10 different strains (OTUs) of *Microcystis* over the study period. Four of these strains (#OTUs 1, 2, 3 and 8) were observed in both the 454

analysis and the colony PCR sequences, two of them were only observed in the colony PCR sequences and four were observed only in the 454 pyrosequences (Supporting Information Fig. S3).

A comparison of *Microcystis* OTU relative abundances and QPCR estimates of the toxigenic proportion of *Microcystis* sp. failed to clearly distinguish toxin-producing strains (Fig. 2). The sequencing data indicated the
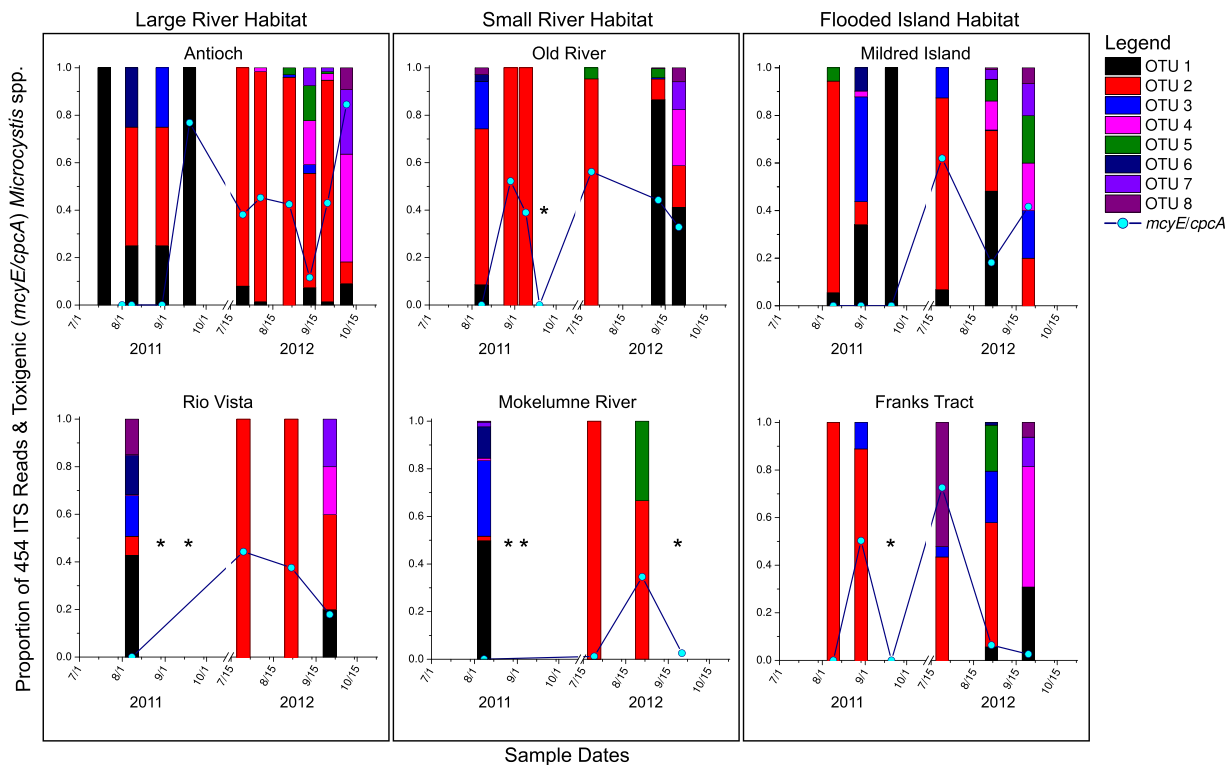
Fig. 2. High throughput 454 pyrosequencing of *Microcystis* spp. 16–23S rRNA ITS region revealed eight distinct operational taxonomic units (OTU) delineated at 97% nucleotide identity; the ratio of *mcyE* to *cpcA* as inferred by QPCR is represented by the blue line. Asterisks (*) denote sample where not enough *Microcystis* was present to sequence. [Colour figure can be viewed at wileyonlinelibrary.com]

presence of at least six microcystin producing strains within the Delta *Microcystis* community (Supporting Information Fig. S4). Our results indicate the presence of multiple *Microcystis* strains within the Delta, several of which are capable of producing microcystin. Genetic analysis of McyB1 and McyC1 modules predicted arginine would be incorporated by McyC1 (Z position) and arginine and leucine into McyB1 (X positions). Based on Stachelhaus codes, five of the six toxigenic strains are expected to support synthesis of MC-RR with the sixth expected to produce MC-LR (Supporting Information Fig. S4 and Supporting Information Table S3).

Identification of other microcystis secondary metabolites

Most cyanobacterial genomes contain multiple NRPS/PKS pathways; a previous analysis of 15 sequenced *Microcystis* sp. genomes revealed on average five NRPS/PKS operons per strain (min = 2, max = 8) (Otten and Paerl, 2015). Several *Microcystis* NRPS/PKS operons were identified in the Mildred Island metagenome assemblies that encode for microcystin, aeruginosin, anabaenopeptin, cyanopeptolin and microginin. It was determined that the aeruginosin operon (*aerAJBCKDEFLGMN*) was likely missing *aerC* and *aerK* genes in a subset of the population

and *aerG2* was totally absent from all strains; the anabaenopeptin operon was intact (*apnA-E* with ORFs1–3), the cyanopeptolin operon was missing *mcnA* (*mcnB-F*), the microcystin operon was intact (*mcyA-J*) and the microginin operon lacked *micB* (*micA-E* with ORFs1–3). Microviridin, piricyclamide and psm3 genes failed to assemble, but all were identified by read mapping to reference genes of these operons (Fig. 3). Note that psm3 is a mixed NRPS/PKS bi-directional operon that has been reported from several *Microcystis* sp. strains (Nishizawa *et al.*, 2007; Humbert *et al.*, 2013), although its product remains uncharacterized. Piricyclamides are a sub-group of structurally diverse cyclic peptides (cyanobactins) that are widely distributed within the genus *Microcystis* (Leikoski *et al.*, 2012). Microviridin is the most common secondary metabolite whose genes have been found in all *Microcystis* sp. genomes investigated to date; however, in this study we were able to assemble only small fragments of the gene cluster. We believe this was due to its presence in several *Microcystis* sp. strains present in the same sample at markedly different read coverage depths which can lead to breaks in the assembly. Rolling coverage estimates of NRPS/PKS operon coverage depths provided an estimate for their relative abundance in the Delta *Microcystis* population (Fig. 3). This approach revealed that microviridin
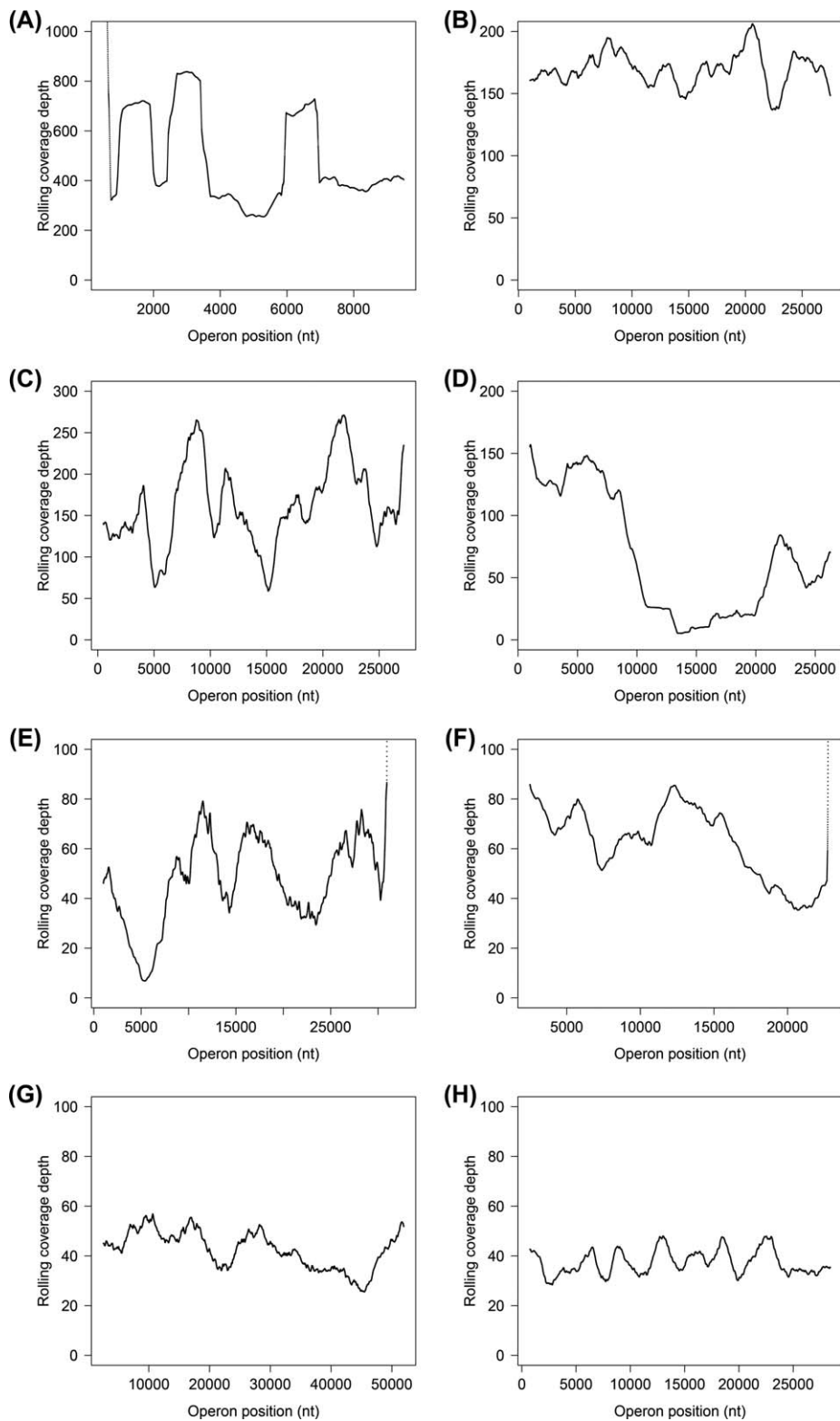
Fig. 3. Read recruitment coverage plots for *Microcystis* secondary metabolites observed in Mildred Island metagenomes; (A) microviridin (AM943877.1), (B) anabaenopeptin (this study), (C) aeruginosin (this study), (D) microginin (DM195384.1), (E) cyanopeptolin (AB481215.1), (F) piriclamide (FJ609416.1), (G) microcystin (AF183408.1), (H) psm3 (AB279593.1)

genes were most abundant ($\mu = 570X$ cov.), followed by anabaenopeptin ($\mu = 168X$ cov.), aeruginosin ($\mu = 163X$ cov.), microginin ($\mu = 140X$ cov.), piriclamide ($\mu = 63X$ cov.), cyanopeptolin ($\mu = 57X$ cov.), microcystin ($\mu = 41X$ cov.) and psm3 ($\mu = 37X$ cov.). Importantly, genes for other freshwater algal biotoxins of public health concern, including: anatoxin-a, cylindrospermopsin and saxitoxin were not observed.

Table 1. Mean (±95% confidence intervals) for water quality variables from all six Delta sites and for Mildred Island individually.

	All (n = 36) 2011	All (n = 36) 2012	MIL (n = 6) 2011	MIL (n = 6) 2012
k	1.14 ± 0.10	1.10 ± 0.10	1.07 ± 0.19	1.28 ± 0.20
Temp	22.3 ± 0.3	21.2 ± 0.4	23.3 ± 0.4	22.2 ± 1.2
Cond	192 ± 51	568 ± 192	168 ± 15	283 ± 58
pH	7.8 ± 0.1	7.9 ± 0.1	7.65 ± 0.14	7.8 ± 0.05
DO	7.2 ± 0.2	7.8 ± 0.2	6.62 ± 0.37	7.46 ± 0.27
DIC	1063 ± 60	1266 ± 47	1024 ± 158	1248 ± 96
SiO$_3$	138 ± 31	232 ± 17	117 ± 70	211 ± 72
NO$_3$	12.3 ± 1.8	11.6 ± 1.9	20.5 ± 2.2	11.0 ± 2.3
NO$_2$	0.41 ± 0.10	0.55 ± 0.14	0.33 ± 0.08	0.37 ± 0.09
PO$_4$	1.71 ± 0.12	1.78 ± 0.10	1.93 ± 0.22	1.92 ± 0.11
NH$_3$	2.85 ± 1.02	3.18 ± 0.99	0.68 ± 0.4	1.35 ± 0.65
Urea	0.28 ± 0.06	0.22 ± 0.06	0.33 ± 0.1	0.23 ± 0.12
Chl a	3.51 ± 0.85	4.93 ± 1.8	3.3 ± 2.2	7.3 ± 4.6
FCM	0.76 ± 0.18	0.74 ± 0.07	1.0 ± 0.8	0.86 ± 0.20

k = light attenuation coefficient; Temp = water temperature (°C); Cond = conductivity (μS cm^{-1}); DO = dissolved oxygen (mg L^{-1}); DIC = dissolved inorganic carbon (μM); SiO$_3$ = silicate (μM); NO$_3$ = nitrate (mg L^{-1}); NO$_2$ = nitrite (mg L^{-1}); PO$_4$ = phosphate (mg L^{-1}); NH3 = ammonia (mg L^{-1}); Urea (mg L^{-1}); Chl a = chlorophyll a (μg L^{-1}); FCM = flow cytometry (10^6 cells L^{-1}).

Analysis of microbial community structure

The QPCR data indicated that the largest *Microcystis* bloom observed over the study period occurred at the Mildred Island sampling site in 2012, peaking around 27 August 2012. The bloom disappeared soon after this date, with *Microcystis* present at only 1570 cell equivalents ml^{-1} 2 weeks later. Microscope observations corroborate the disappearance of *Microcystis*, as no cells were observed from samples collected at 0.2 or 3 m depth on 10 September 2012 (Supporting Information Fig. S5). The environmental data (Table 1) provided no obvious explanation for a sudden collapse (e.g., weather events or a change in water chemistry), suggesting that the bloom had either passively moved to another location, gone dormant (i.e., settled out of the water column) or had collapsed as a result of top-down controls (e.g., cyanophage, predatory bacteria or zooplankton grazers). Shotgun metagenomes from three Mildred Island samples corresponding to pre-bloom, peak-bloom and post-bloom conditions were analysed in order to screen for potential top-down control agents and to investigate how microbial community structure may vary at different stages of a cyanobacterial bloom. Covariance in contig coverage depth was used to cluster contigs in 2D space (Albertsen *et al.*, 2013), with tight concentric clusters representative of single strains (Fig. 4). Some organisms exhibited 'contig smearing', which is thought to be caused by shared genes between closely related, co-occurring strains present in different abundances (Daims *et al.*, 2015). For example, many bacterial and phage genomes formed relatively tight, concentric groupings, whereas the *Microcystis* contigs were spread both laterally and vertically (Fig. 4), owing to the presence of multiple *Microcystis* strains within the population. Contigs situated along the grey diagonal line represent relatively unchanged organismal abundances across the dates compared. This analysis yielded several important observations: (1) *Microcystis* appeared to be the single most abundant taxon present during the bloom, with coverage depths ranging from 20 to 250×; (2) numerous known and putative bacteriophages represented the second most abundant entities based on coverage depth; (3) *Pseudanabaena* and *Synechococcus* were most abundant when *Microcystis* was most abundant; (4) an unidentified Verrucomicrobia cluster and *Candidatus Aquiluna* sp. appeared to increase in response to the *Microcystis* bloom suggesting a possible synergistic or mutualistic relationship; (5) a greater number of contigs were located to the right than to the left of the 1:1 ratio line in Fig. 4, suggesting that fewer taxa were present during the bloom than either before or after the bloom.

By recruiting *de novo* assembled contigs to known *Microcystis* cyanomyophage genomes (the closely related Ma-LMM01 and MaMV-DC) (Yoshida *et al.*, 2008; Ou *et al.*, 2015), eight non-overlapping contigs spanning 166 477 bp were identified. For reference, the genome lengths of Ma-LMM01 and MaMV-DC are 162 109 and 169 223 bp, respectively, suggesting that these eight contigs likely represented most of the genome of a related phage (89%–96% nucleotide similarity; Supporting Information Table S4). The putative *Microcystis* phage had mean read coverage depths of 0.15X, 17.0X and 0.48X across the time-series, whereas mean *Microcystis* read coverage depths of contigs containing essential genes were 7.9X, 163.6X and 0.41X respectively. The co-occurrence of multiple *Microcystis* strains and their independent flexible genomes complicates coverage estimates, which is why contigs containing essential genes were used in these estimates of relative abundance.

The Nonpareil curves indicated the 23 July 2012 sample sequencing effort of 2.51 giga base pairs (Gbp) represented an estimated 89.4% of the microbial community, the 27 August 2012 sample sequencing effort of 1.94 Gbp represented 93.1% of the microbial community, and the 10 September 2012 sample sequencing effort of 3.91 Gbp represented 99.8% of the microbial community (Fig. 5A). These data indicated that even though the *Microcystis* bloom on 27 August was numerically dominant, it did not severely compromise our ability to detect and quantify the majority of other bacterial genomes comprising the sample. Further, the Nonpareil curve for 27 August was shifted significantly to the left, indicating that the sample was less diverse than the other two samples since the curve became asymptotic with fewer sequencing reads. In order to further assess if recruitment bias explained the
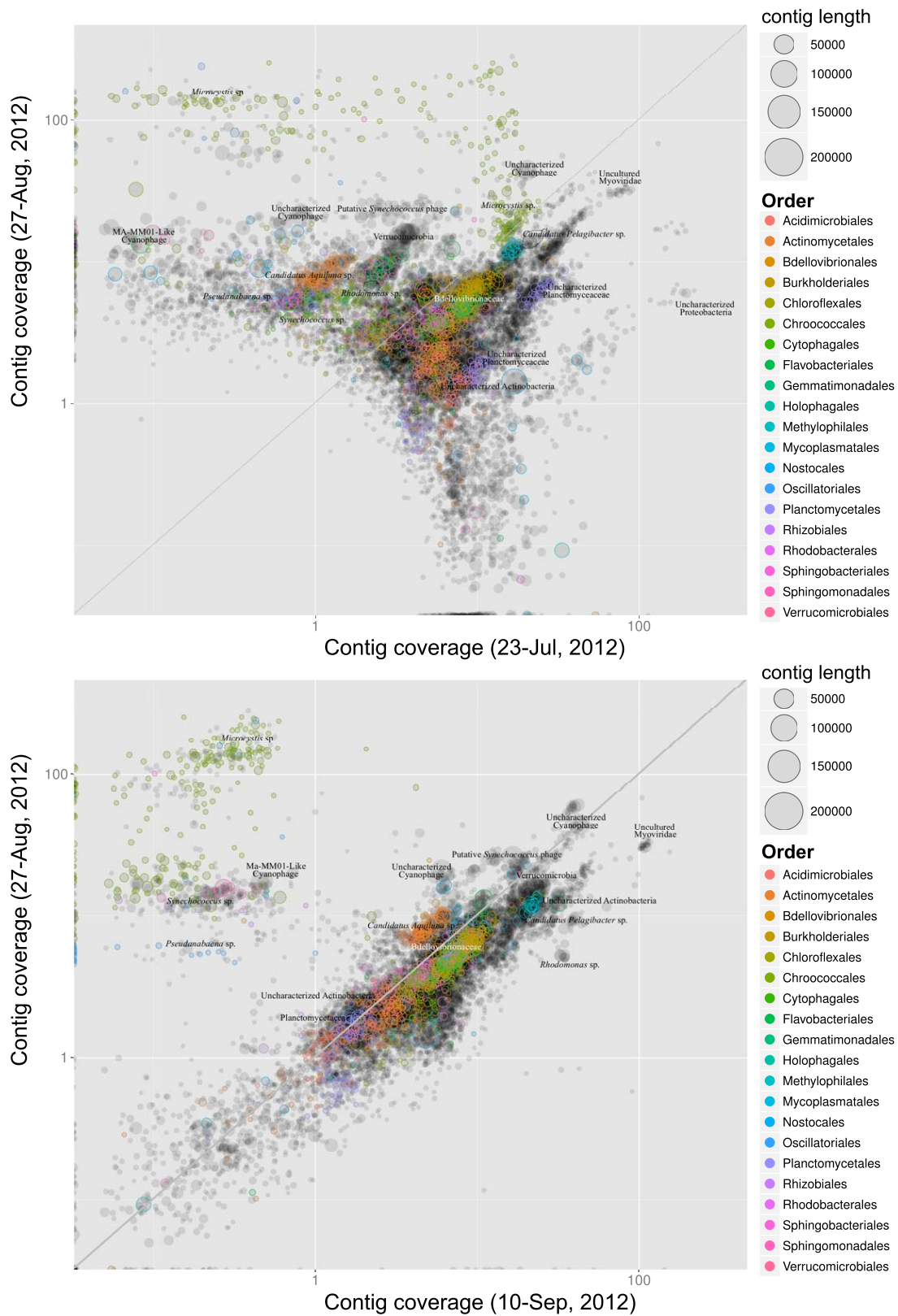
Fig. 4. Assessment of bacterial community structure and relative abundance before (23-July), during (28-Aug) and after (10-Sept) a *Microcystis* spp. bloom at Mildred Island in 2012. Contig lengths and their average coverage depths are displayed. Contigs along the grey line are uniformly represented between the compared time points. Note: only contigs longer than 3 kbp are displayed. [Colour figure can be viewed at wileyonlinelibrary.com]
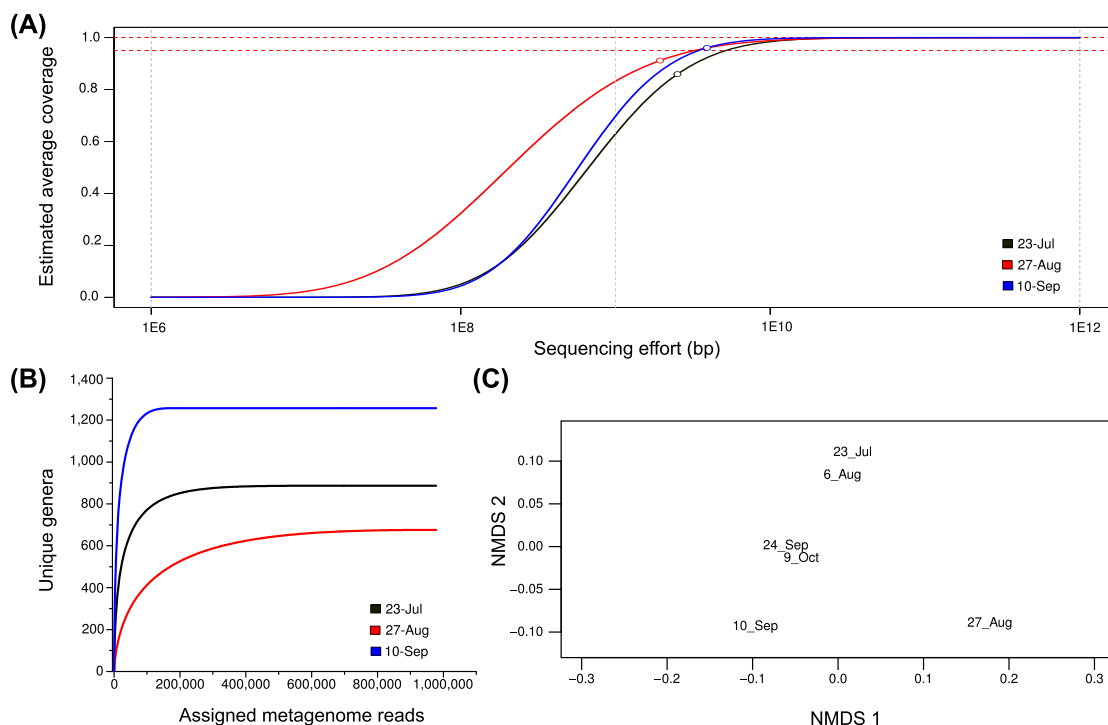
Fig. 5. (A) Nonpareil curves estimating the average coverage (completeness) of Mildred Island metagenomic datasets conducted on 2012 samples and corresponding to pre-, peak- and post-*Microcystis* bloom (black, red and blue, respectively); empty circles denote the actual sequencing effort (bp of sequence), dashed red lines indicate sequencing effort needed for 95% and 100% community coverage. (B) Estimation of community richness (# of unique genera) by rarefaction curve analysis calculated from a normalized subset of protein-encoding sequences. (C) Non-metric multidimensional scaling analysis (NMDS) displaying Mildred Island microbial community composition by date (2012), based on bacterial 16S rRNA OTUs (97% identity). [Colour figure can be viewed at wileyonlinelibrary.com]

apparent antagonistic relationship between *Microcystis* abundance and the majority of other contigs, an assembly-free rarefaction assessment was employed. The results indicated that the sequencing depth of each sample was appropriate to reach saturation (Fig. 5B). This analysis again revealed considerably fewer genera present in the sample collected during the *Microcystis* bloom (676 genera) relative to pre-bloom (887 genera) and post-bloom (1257 genera) conditions, which corresponded to Shannon's Diversity (*H'*) estimates of 2.32, 0.61 and 3.71 respectively. Combined, these data indicate that a significant loss in microbial biodiversity occurred during the *Microcystis* bloom, and this inference is not due to proportional biases inherent to sequencing assembly or assignment.

In order to further assess how bacterial community structure differed before, during and after the *Microcystis* bloom, changes in community structure were inferred by non-metric multidimensional scaling analysis (NMDS) on 16S rRNA reads collected across each of the six Mildred Island samples collected in 2012. On the basis of assigned bacterial genera and their rank abundances, samples collected prior to the bloom (23 July and 6 August) were closely related in composition. The bloom

sample (27 August) and immediate post-bloom sample (10 September) had distinct compositions from the other dates, while the last two samples (24 September and 9 October) clustered together and trended toward the pre-bloom community structure (Fig. 5C).

Network (co-occurrence) analysis was applied to further assess how bacterial community structure responded to the *Microcystis* bloom based on covariance patterns of the 16S rRNA OTUs (Table 2). *Microcystis* was positively correlated with OTUs corresponding to *Pseudanabaena* (Cyanobacteria), *Anabaena* (Cyanobacteria), *Phenylobacterium* (Alphaproteobacteria), *Hyphomonadaceae* (Alphaproteobacteria), *Ramlibacter* (Betaproteobacteria) and *Peredibacter* (Deltaproteobacteria) and it was negatively correlated with *Smithella* (Deltaproteobacteria), *Limnobacter* (Betaproteobacteria), *Stenothermobacter* (Bacteroidetes), an unidentified *Erythrobacter* (Alphaproteobacteria), a member of the Beijerinckiaceae (Alphaproteobacteria) and an unidentified cyanobacterium (Table 2; Supporting Information Fig. S6).

Discussion

This study utilized a suite of molecular and physicochemical analyses in an effort to better understand the

Table 2. Microbial co-occurrence (network) analysis based on covariance of 16S rRNA OTU groupings for Mildred Island 2012 samples ($n = 6$); only significant ($p < 0.05$), strongly positive ($r > 0.75$) and negative ($r < -0.75$) *Microcystis* sp. interactions are shown, the false-discovery rate (q-value) is provided.

OTU 1	OTU 2 (Phylum)	rho	p-value	q-value
Microcystis	*Pseudanabaena* (Cyanobacteria)	0.955	0.003	0.0002
Microcystis	*Anabaena* (Cyanobacteria)	0.893	0.016	0.0010
Microcystis	*Phenylobacterium* (Alphaproteobacteria)	0.857	0.029	0.0015
Microcystis	*Hyphomonadaceae* (Alphaproteobacteria)	0.857	0.029	0.0015
Microcystis	*Ramlibacter* (Betaproteobacteria)	0.857	0.029	0.0015
Microcystis	*Peredibacter* (Deltaproteobacteria)	0.851	0.032	0.0016
Microcystis	*Limnobacter* (Betaproteobacteria)	-0.897	0.015	0.0057
Microcystis	*Erythrobacter* (Alphaproteobacteria)	-0.892	0.017	0.0057
Microcystis	*Smithella* (Deltaproteobacteria)	-0.882	0.020	0.0057
Microcystis	*Unidentified* Cyanobacterium	-0.840	0.036	0.0058
Microcystis	*Stenothermobacter* (Flavobacteriia)	-0.823	0.044	0.0058
Microcystis	*Beijerinckiaceae* (Alphaproteobacteria)	-0.821	0.045	0.0058

ecological implications of *Microcystis* blooms within the SFE Delta. *Microcystis* blooms were prevalent in 2012 at the flooded island sites (Franks Tract and Mildred Island) and also in Old River which is near Discovery Bay – an enclosed marina prone to *Microcystis* blooms. On the contrary, unlike the previous several years when *Microcystis* sp. was the most prevalent cyanobacterium (Baxa *et al.*, 2010), the phytoplankton community was dominated by *Aphanizomenon flos-aquae* during the 2011 sampling season. In an effort to elucidate the environmental conditions favouring *Microcystis* growth over other taxa, we compared all physicochemical data from all sites between the 2 years and for Mildred Island individually since that was where the largest *Microcystis* bloom was observed over the study period. Unexpectedly, water temperatures were found to be higher on average in 2011 than during the drought in 2012. Conductivity, dissolved inorganic carbon (DIC) and silicate (SiO_3) were all significantly higher in 2012 when *Microcystis* was the dominant cyanobacterium throughout the system. All three of these metrics are likely a consequence of longer residence times throughout the Delta as a result of the drought conditions in 2012. During both study years inorganic nitrogen and phosphate concentrations were well above growth limiting concentrations, suggesting that water residence time may be the main environmental driver of *Microcystis* blooms within the Delta (Paerl and Otten, 2013; Paerl and Otten, 2016) (Table 3).

Prior to this study, only a few investigations had incorporated molecular tools in characterizing Delta cyanobacterial blooms. Baxa *et al.* (2010) used QPCR to estimate the abundance and proportion of toxigenic *Microcystis* throughout the Delta in a 2007 study. They reported that the percentage of toxigenic (*mcyA* copies) *Microcystis* relative to total *Microcystis* (16S rRNA copies) ranged from 0% to 27%. Here we estimated the percentage of toxigenic *Microcystis* to range from 0% to 84% ($\mu = 26\%$) based on single copy microcystin (*mcyE*) and phycocyanin (*cpcA*) genes as opposed to 16S rRNA genes, which based on the strains of *Microcystis* sequenced to date occur in duplicate in the genome. Seasonality may influence estimates of toxigenicity, since the percentage of toxigenic cells relative to total *Microcystis* tends to vary over the course of the

Table 3. Relative abundance (percentage of 16S rRNA reads) represented by each bacterial phylum from Mildred Island (2012).

Bacteria (Phylum)	23-Jul	6-Aug	27-Aug	10-Sep	24-Sep	9-Oct
Acidobacteria	0.60	2.07	1.23	1.77	2.63	1.34
Actinobacteria	31.85	14.32	8.83	16.81	13.37	20.06
Bacteroidetes	22.17	33.61	14.85	23.31	29.55	13.28
Chlamydiae	0.00	0.00	0.13	0.00	0.00	0.00
Chlorobi	0.53	0.26	0.36	0.23	0.17	0.44
Chloroflexi	0.09	0.22	0.16	0.70	0.56	0.63
Cyanobacteria	10.98	10.88	40.35	19.86	11.55	17.65
Firmicutes	0.00	0.31	0.21	0.05	0.08	0.15
Gemmatimonadetes	0.05	0.37	0.37	0.43	0.58	0.22
Planctomycetes	0.85	0.25	1.32	1.31	0.78	2.05
Proteobacteria	28.30	33.11	27.03	31.06	34.88	40.73
Verrucomicrobia	2.68	2.80	0.94	2.77	3.91	1.62
Unassigned/other	1.90	1.81	4.21	1.73	1.93	1.81

season, often with higher percentages of toxigenic cells earlier in the summer with nontoxic variants dominating in the late fall (Bozarth *et al.*, 2010).

Regarding *Microcystis* strain diversity within the Delta, a previous study using Sanger sequenced clone libraries of *cpcBA* ($n = 148$ reads) and *mcyA* ($n = 124$ reads) gene sequences identified the presence of three strains (OTUs) of *Microcystis* (Moisander *et al.*, 2009). With the high throughput methods now available, we have shown that the Delta *Microcystis* population comprises at least 10 strains based on 16S-23S rRNA amplicon sequences. This community includes at least six distinct microcystin-producing strains. However, the weak relationships between 16S-23S rRNA derived OTUs, *mcyB* genotypes and QPCR derived estimates of toxigenicity suggest little linkage between the 16S-23S rRNA locus and microcystin potential. Instead, the microcystin operon appears to be widely distributed across *Microcystis* lineages within the Delta.

On the basis of amino acid adenylation domain binding pocket signatures, a variety of *Microcystis* strains in the Delta appear to be capable of synthesizing the microcystin variant MC-RR, with MC-LR specific genes also present. However, because multiple microcystin variants have been observed from single strains of *Microcystis* (Puddick *et al.*, 2014), likely due to a lack of specificity at the McyB1 adenylation domain (Fewer *et al.*, 2007), the presence of congeners other than those predicted cannot be determined genetically. A previous study found MC-LR to be the most common variant in the Delta, comprising $\sim 54\%$ of total microcystins, with MC-FR, MC-WR, MC-LA and other undetermined variants comprising the remainder (Lehman *et al.*, 2008). Microcystin congeners are important because different ones carry different public health risks; for example, MC-LR is 6.4-fold more toxic than MC-RR and 8.4-fold more toxic than [Dha[7]]MC-RR in mice (Chen *et al.*, 2006; Gupta *et al.*, 2003).

Microcystis and the pelagic organism decline

The concomitant appearance of *Microcystis* sp. blooms with the collapse of several fish populations in the SFE beginning in the early 2000s raised the possibility that cyanobacterial blooms may have contributed to their decline. In order to better understand the physicochemical or biological drivers of this decline, we sought first to characterize the ecology and physiology of the Delta *Microcystis*-microbial community. If *Microcystis* blooms negatively influence fish or zooplankton survival, then these effects are likely episodic throughout the Delta, since *Microcystis* was not prevalent in 2011 and it is generally absent from certain regions such as the Sacramento River at Rio Vista and in the Mokelumne River. Further, it is highly unlikely that *Microcystis* blooms represent the only

stressor to mobile fishes or the zooplankton that they prey upon. However, the magnitude and persistence of these blooms suggests that when present they have the potential to influence food web structure widely throughout the SFE Delta, including areas of high salinity, based on the presence of elevated microcystins in marine bivalve tissue in San Francisco Bay (Gibble *et al.*, 2016). In this study, we observed a significant reduction in microbial community diversity around the peak of a *Microcystis* bloom in Mildred Island in 2012 when community richness was reduced by $\sim 25\%$ and $\sim 46\%$ relative to pre- and post-bloom periods respectively. A variety of mechanisms could contribute to a decrease in microbial diversity during a bloom, such as: (1) bloom photosynthesis and respiration may alter water quality (e.g., high dissolved oxygen or reactive oxygen species, high pH, low nutrients, etc.) to the detriment of sensitive taxa; (2) alteration of the community due to mixing or flushing; (3) resource competition or (4) the production of broad allelopathic compounds by *Microcystis* sp. could impair the fitness of other bacterial or eukaryotic taxa.

We considered whether *Microcystis* blooms could broadly and indirectly influence microbial structure by altering the physicochemical properties of the water column. During cyanobacterial bloom events, the epilimnion often becomes supersaturated with oxygen and pH levels may exceed 10 units due to high photosynthetic activity; these conditions are likely deleterious for certain microbial taxa (Spietz *et al.*, 2015; Zeglin, 2015). However, the Delta is shallow and tidally mixed which generally precludes stratification and large swings in water chemistry. At Mildred Island in 2012, dissolved oxygen concentrations ranged from 7.04 to 7.8 mg L^{-1} and pH ranged from 7.46 to 7.81, both of which are moderate values unlikely to cause a major loss in microbial biodiversity (Hansen, 2002; Liu *et al.*, 2015). Additionally, water temperatures were relatively stable, ranging from 20.9°C to 24.3°C (23.1°C at peak bloom) and dissolved total nitrogen and phosphorus (DTN:DTP) ratios remained low, ranging from 4.7 to 8.3. The collapse of the *Microcystis* bloom was followed by a 43% increase in dissolved total nitrogen (mostly NO_3^-) during the following transect. Because the bloom dissipated at some point during a 12 day span between sampling trips, it cannot be determined if the increase in DIN was due to bloom lysis (which would have released predominantly NH_4^+ and DON) and subsequent nitrification into NO_3^-, or if the increase in NO_3^- was due to relaxation of biological nitrogen demand following bloom termination.

Strong tidal flows in the spatially reticulate Delta make flow patterns complex. The low microbial diversity observed during the bloom could have been due to advection or tidal mixing of a different microbial assemblage into Mildred Island rather than *in situ* community succession processes. Hydrodynamic flushing time at Mildred Island under dry conditions is ~ 8 days (Monsen *et al.*, 2002) and

is mostly a function of tidal flows (Monsen *et al.*, 2002); under these conditions most of the water drawn through Mildred Island originates from the Sacramento River. If microbial community structure at Mildred Island was strongly influenced by that in the Sacramento River, then microbial assemblages should be similar between Mildred Island and Rio Vista, and to a lesser extent, Antioch. As inferred by the 16S-23S rRNA sequencing, the *Microcystis* community at both Rio Vista and Antioch consisted entirely of OTU2 during this period, whereas at Mildred Island there were never fewer than three strains present and OTU1 was the dominant *Microcystis* strain. These results suggest that flushing rates through Mildred Island were not so high as to preclude the growth of autochthonous microbial populations and that changes in microbial community structure were more likely to be driven by internal processes than by physical transport.

The increasing relative abundance of a putative *Microcystis* cyanomyophage leading up to the collapse of the bloom, but absent thereafter, indicated a role for top–down control of the bloom as opposed to its physical dispersal. Viral lysis of the filamentous cyanobacterium *Oscillatoria* sp. has been observed to result in a concomitant increase in microbial species richness, with those bacterial taxa capable of degrading large, complex carbohydrates, such as members of the Cytophagales and Actinobacteria, increasing the most (Van Hannen *et al.*, 1999). In this study, nutrient concentrations overall remained relatively stable, although they were elevated in the sample collected at Mildred Island following bloom collapse. This post-bloom sample also had the greatest microbial diversity (Fig. 5), suggesting that the community may have responded positively to the augmented nutrient pool and presumed release of dissolved organic carbon into the water column.

In the absence of a biologically plausible environmental explanation for the reduction in microbial community diversity during the bloom, we considered whether this pattern may be explained by resource competition. To date, no consistent relationship between freshwater primary productivity gradients and microbial diversity has emerged from the literature. Some studies have reported there to be no relationship between diversity and productivity, whereas others have noted positive or negative relationships, or peak diversity occurring at intermediate productivity (Horner-Devine *et al.*, 2003). A particularly relevant comparison to our study is a recently published time-series analysis of microbial community structure spanning a series of cyanobacterial successions in an Australian lake (Woodhouse *et al.*, 2016). In that study, the authors reported that the microbial community changed dependent on the dominant cyanobacterial genus present, but also that bacterial community diversity (based on Simpson's index) was positively correlated with cyanobacterial abundance. These findings are in contrast to the current study,

suggesting that strain-specific interactions, as opposed to broad effects consistent with all cyanobacterial blooms (e.g., autochthonous organic carbon production) are important forces in shaping the microbial taxa that coexist with cyanobacteria.

Using network analysis we were able to evaluate putative taxon-specific microbial interactions with *Microcystis*. Based on previous studies of the 'phycosphere' (Bell and Mitchell, 1972; Potts 1973), it was expected that heterotrophic bacteria would be tightly coupled with *Microcystis* distributions. For instance, Parveen *et al*. (2013) observed that bacteria attached to *Microcystis* colonies were depleted in Actinobacteria and enriched in Gammaproteobacteria, especially during bloom decline. Louati *et al*. (2015) reported Betaproteobacteria to be positively and Actinobacteria negatively associated with both *Microcystis* and *Anabaena* blooms, while Nitrosomonadales were associated with *Microcystis*, and Verrucomicrobia with *Anabaena*. Bagatini *et al*. (2014) likewise observed commonalities, differences and growth phase dependencies in bacterial groups associated with *Microcystis* or *Cylindrospermopsis*. Bacteria are believed to associate with phytoplankton in order to access labile organic carbon, nitrogen or other exuded photosynthates, and in the case of cyanobacterial blooms, the polysaccharides comprising the mucilaginous sheath of colonies. In return, photoautotrophs could benefit from recycled nutrients, vitamins and services such as siderophores or antioxidant provision (c.f., Paerl and Millie, 1996; Amin *et al*., 2012). Our study allowed the identification of associations with bacteria at finer taxonomic scales than earlier reports, including genus assignments when possible. This revealed both negative and positive associations with different Alphaproteobacteria, Betaproteobacteria and Deltaproteobacteria. The broader implications of these interactions are at present unknown, but the existence of such interactions seen in our study and in the literature support the contention that *Microcystis* blooms are responsible for reshaping at least part of the microbial community.

Even though there was a sizable reduction in the number of bacterial OTUs during the bloom, and the relative contributions of non-cyanobacteria to the overall community were decreased during the bloom, there were no drastic changes in the rank order of bacterial phyla. This suggested that the decrease in OTUs during the bloom was counterbalanced by a relative increase in specific taxa from each phylum, as illustrated by the within-phylum positive and negative interactions discussed above. Because size-fractionated particulate organic carbon was not measured in this study, it is unclear if the decrease in microbial diversity was accompanied by an overall decrease in bacterial biomass, or if the vacated niches were in turn filled by superior competitors or specialists. OTUs not correlated with *Microcystis*, yet increasing the most over the bloom

period (possibly driven by other environmental factors), included: Myxococcales (δ-proteobacteria), *Pirellula* sp. (Planctomycetales), *Flavobacterium* sp. (Bacteroidetes), Rhodobacteraceae (α-proteobacteria), *Planctomyces* sp. (Planctomycetes), Acidimicrobiaceae (Actinobacteria) and *Gemmatimonas* sp. (Gemmatimonadetes). At the phylum level, only Actinobacteria and Bacteroidetes declined in relative abundance during the bloom, suggesting that these two groups were more negatively influenced by *Microcystis* blooms than other bacterial phyla. While other studies have observed negative correlations between Actinobacteria and Cyanobacteria (Steffen *et al.*, 2012; Parveen *et al.*, 2013; Louati *et al.*, 2015; Woodhouse *et al.*, 2016), they also reported positive associations between Bacteroidetes taxa and Cyanobacteria. Out of all OTUs assigned to the phylum Bacteroidetes, only members of the Flavobacteriales were observed to increase during the bloom. This pattern was also observed in the shotgun metagenomes where the average coverage depth of contigs annotated as Flavobacteriaceae doubled during the bloom. Previous studies have shown *Flavobacterium* sp. to enhance growth of *Microcystis* sp. and that members of this genus are able to cyanobacterial toxins and other complex organic compounds (Berg *et al.*, 2009).

Implications of identified microcystis secondary metabolites

Cyanobacteria are well recognized to produce a large variety of novel bioactive and allelopathic metabolites (Kehr *et al.*, 2011), many of which are believed to exert negative effects on a range of microbes and plankton (Granéli *et al.*, 2008). Detailed analysis of the *Microcystis* genomes recovered from the shotgun metagenomes identified the presence of at least eight secondary metabolite gene clusters. To our knowledge, there have been no studies that address how cyanobacterial secondary metabolites may influence bacterial communities, although there have been numerous studies on allelopathy between phytoplankton and zooplankton groups. One such secondary metabolite worthy of further study is microviridin, as the genes for this metabolite were present in the greatest relative abundance out of all *Microcystis* secondary metabolite pathways identified in this study. This is probably due to their ubiquity in all *Microcystis* genomes ($n = 17$) that have been sequenced to date. Not only are microviridin genes seemingly present in all *Microcystis* genomes, they were also some of the most highly expressed genes in the aquatic environment during a metatranscriptomic study of a *Microcystis* bloom (Penn *et al.*, 2014). This suggests that microviridin may play a central role in *Microcystis* physiology. The authors of the metatranscriptome study speculated that microviridin may function as an antigrazing compound. The study also revealed that

Microcystis was the principal source for transcripts of NRPS/PKS gene clusters and that microcystin and aeruginosin were actively expressed throughout the day–night cycle.

Previous studies investigating the effects of dietary *Microcystis aeruginosa* on the dominant zooplankters in the Delta have indicated that *Eurytemora affinis* is more negatively influenced by *Microcystis* than *Pseudodiaptomus forbesi*, and that the latter was not as affected by an MC+ *M. aeruginosa* strain (UTEX2385) as by an MC- *M. aeruginosa* strain (UTEX2386) (Ger *et al.*, 2010). Therefore, metabolites other than microcystin are likely toxic to copepods. Cyanobacterial secondary metabolites may thus indirectly influence POD-impacted fishes, since calanoid copepods are the key prey of their larvae (Slater and Baxter, 2014). PCR assays targeting *Microcystis* genes involved in the biosynthesis of aeruginosin, cyanopeptolin, micropeptin, microviridin and piriciclamide (*aerB*, *cpnC*, *mpnC*, *mvdB*, *pirA*, respectively), were run on the UTEX2386 strain used in the feeding experiment (Ger *et al.*, 2010). The results indicated that UTEX2386, while not a microcystin producer, has genes involved in cyanopeptolin, micropeptin and microviridin biosynthesis (Supporting Information Fig. S7). Acknowledging that other secondary metabolites may also be present, and assuming that all *Microcystis* strains produce microviridin, these results indicate that future studies should investigate the role of cyanopeptolin and micropeptin on the survival and fitness of *P. forbesi* and *E. affinis*. Future studies should also recognize that there are a number of different cyanopeptolin variants that may exhibit different toxicological characteristics (Czarnecki *et al.*, 2006). Cyanopeptolins have been purified and identified as serine protease inhibitors that interfere with digestion physiology in the cladocerans *Daphnia magna* and *Moina macrocopa* (Agrawal *et al.*, 2001; von Elert *et al.*, 2004). Similarly, aeruginosins and microviridins have been shown to inhibit proteases (Welker and von Döhren, 2006), and microviridin J can induce a lethal molting disruption in *Daphnia pulicaria* (Rohrlack *et al.*, 2004). Aside from microcystins, which seem to produce variable effects on zooplankton consumers, the effects of other secondary metabolites on zooplankton have been assessed in only a few toxicology studies, and even fewer studies address the calanoid copepods that are critical components of the Delta food web.

Conclusions

In this study we provide evidence that aquatic microbial diversity was significantly reduced during a *Microcystis* bloom. The effect that this may have on the microbial loop and the transfer of energy throughout the food web remains unresolved. In addition to microcystin, we identified a number of *Microcystis* secondary metabolites that

have been found to exert allelopathic effects on bacterioplankton and/or zooplankton. A better understanding of how cyanobacterial blooms and their secondary metabolites influence aquatic ecosystems is warranted.

References

Acuña, S., Deng, D.F., Lehman, P., and Teh, S. (2012) Sublethal dietary effects of *Microcystis* on Sacramento splittail, *Pogonichthys macrolepidotus*. *Aquat Toxicol* **110–111:** 1–8.

Albertsen, M., Hugenholtz, P., Skarshewski, A., Tyson, G.W., Nielsen, K.L., and Nielsen, P.H. (2013) Genome sequences of rare, uncultured bacteria obtained by differential coverage binning of multiple metagenomes. *Nat Biotechnol* **31:** 533–538.

Agrawal, M.K., Bagchi, D., and Bagchi, S.N. (2001) Acute inhibition of protease and suppression of growth in zooplankter, *Moina macrocopa*, by *Microcystis* blooms collected in Central India. *Hydrobiologia* **464:** 37–44.

Alpine, A.E., and Cloern, J.E. (1992) Trophic interactions and direct physical effects control phytoplankton biomass and production in an estuary. *Limnol Oceanogr* **37:** 946–955.

Amé, A.V., Echenique, J.R., Pflugmacher, S., and Wunderlin, D.A. (2006) Degradation of microcystin-RR by *Sphingomonas* sp. CBA4 isolated from San Roque reservoir (Córdoba-Argentina). *Biodegradation* **17:** 447–455.

Amin, S.A., Parker, M.S., and Armbrust, E.V. (2012) Interactions between Diatoms and Bacteria. *Microbiol Mol Bio Rev* **76:** 667–684.

Auer, B., Elzer, U., and Arndt, H. (2004) Comparison of pelagic food webs in lakes along a trophic gradient and with seasonal aspects: influence of resource and predation. *J Plankton Res* **26:** 697–709.

Azam, F., Fenchel, T., Field, F.G., Gray, J.S., Meyer-Reil, L.A., and Thingstad, F. (1983) The ecological role of water-column microbes in the sea. *Mar Ecol Prog Ser* **10:** 257–263.

Bagatini, I.L., Eiler, A., Bertilsson, S., Klaveness, D., Tessarolli, L.P., and Vieira, A.A.H. (2014) Host-specificity and dynamics in bacterial communities associated with bloom-forming freshwater phytoplankton. *PLoS One* **9:** e85950.

Baxa, D.V., Kurobe, T., Ger, K.A., Lehman, P.W., and Teh, S.J. (2010) Estimating the abundance of toxic *Microcystis* in the San Francisco Estuary using quantitative real-time PCR. *Harmful Algae* **9:** 342–349.

Bec, A., Martin-Creuzburg, D., and von Elert, E. (2006) Trophic upgrading of autotrophic picoplankton by the heterotrophic nanoflagellate *Paraphysomonas* sp. *Limnol Oceanogr* **51:** 1699–1707.

Bell, W., and Mitchell, R. (1972) Chemotactic and growth responses of marine bacteria to algal extra cellular products. *Bio Bull* **143:** 265–277.

Berg, K.A., Lyra, C., Sivonen, K., Paulin, L., Suomalainen, S., Tuomi, P., and Rapala, J. (2009) High diversity of cultivable heterotrophic bacteria in association with cyanobacterial water blooms. *ISME J* **3:** 314–325.

Blin, K., Medema, M.H., Kazempour, D., Fischbach, M.A., Breitling, R., Takano, E., and Weber, T. (2013) antiSMASH 2.0 – a versatile platform for genome mining of secondary metabolite producers. *Nucleic Acids Res* **41:** W204–W212.

Bolger, A.M., Lohse, M., and Usadel, B. (2014) Trimmomatic: a flexible trimmer for Illumina sequence data. *Bioinformatics* **30:** 2114–2120.

Bouley, P., and Kimmerer, W.J. (2006) Ecology of a highly abundant, introduced cyclopoid copepod in a temperate estuary. *Mar Ecol Progr Ser* **324:** 219–228.

Bozarth, C.S., Schwartz, A.D., Shepardson, J.W., Colwell, F.S., and Dreher, T.W. (2010) Population turnover in a *Microcystis* bloom results in predominantly nontoxigenic variants late in the season. *Appl Environ Microbiol* **76:** 5207–5213.

Brooks, M.L., Fleishman, E., Brown, L.R., Lehman, P.W., Werner, I., Scholz, N., *et al.* (2012) Life Histories, salinity zones, and sublethal contributions of contaminants to pelagic fish declines illustrated with a case study of San Francisco Estuary, California, USA. *Estuar Coasts* **35:** 603–621.

Burnsd, C.W., and Hegarty, B. (1994) Diet selection by copepods in the presence of cyanobacteria. *J Plankton Res* **16:** 1671–1690.

Caporaso, J.G., Lauber, C.L., Walters, W.A., Berg-Lyons, D., Huntley, J., Fierer, N., *et al.* (2012) Ultra-high-throughput microbial community analysis on the Illumina HiSeq and MiSeq platforms. *ISME J* **6:** 1621–1624.

Chen, Y.M., Lee, T.H., Lee, S.J., Huang, H.B., Huang, R., and Chou, H.N. (2006) Comparison of protein phosphatase inhibition activities and mouse toxicities of microcystins. *Toxicon* **47:** 742–746.

Christoffersen, K., Riemann, B., Hansen, L.R., Klysner, A., and Sørensen, H.B. (1990) Qualitative importance of the microbial loop and plankton community structure in a eutrophic lake during a bloom of cyanobacteria. *Microb Ecol* **20:** 253–272.

Cole, J.J. (1982) Interaction between bacteria and algae in aquatic ecosystems. *Annu Rev Ecol Syst* **13:** 291–314.

Czarnecki, O., Henning, M., Lippert, I., and Welker, M. (2006) Identification of peptide metabolites of *Microcystis* (Cyanobacteria) that inhibit trypsin-like activity in planktonic herbivorous *Daphnia* (Cladocera). *Environ Microbiol* **8:** 77–87.

Daims, H., Lebedeva, E.V., Pjevac, P., Han, P., Herbold, C., Albertsen, M., *et al.* (2015) Complete nitrification by *Nitrospira* bacteria. *Nature* **528:** 504–509.

Ferrão-Filho, A.S., Azevedo, S.M., and DeMott, W.R. (2000) Effects of toxic and non-toxic cyanobacteria on the life history of tropical and temperate cladocerans. *Freshwater Biol* **45:** 1–19.

Fewer, D.P., Rouhiainen, L., Jokela, J., Wahlsten, M., Laaksso, K., Wang, H., and Sivonen, K. (2007) Recurrent adenylation domain replacement in the microcystin synthetase gene cluster. *BMC Evol Biol* **7:** 183.

Feyrer, F., Nobriga, M.L., and Sommer, T.R. (2007) Multidecadal trends for three declining fish species: habitat patterns and mechanisms in the San Francisco Estuary, California, USA. *Can J Fish Aquat Sci* **64:** 723–734.

Ger, K.A., Teh, S.J., Baxa, D.V., Lesmeister, S., and Goldman, C.R. (2010) The effects of dietary *Microcystis aeruginosa* and microcystin on the copepods of the upper San Francisco Estuary. *Freshwater Biol* **55:** 1548–1559.

Gibble, C.M., Peacock, M.B., and Kudela, R.M. (2016) Evidence of freshwater algal toxins in marine shellfish: implications for human and aquatic health. *Harmful Algae* **59:** 59–66.

Gifford, S.M., Rollwagen-Bollens, G., and Bollens, S.M. (2007) Mesozooplankton omnivory in the upper San Francisco Estuary. *Mar Ecol Prog Ser* **348:** 33–46.

Granéli, E., Weberg, M., and Salomon, P.S. (2008) Harmful algal blooms of allelopathic microalgal species: the role of eutrophication. *Harmful Algae* **8:** 94–102.

Gupta, N., Pant, S.C., Vijayaraghavan, R., and Rao, P.V. (2003) Comparative toxicity evaluation of cyanobacterial cyclic peptide toxin microcystin variants (LR, RR, YR) in mice. *Toxicology* **188:** 285–296.

Hammock, B.G., Hobbs, J.A., Slater, S.B., Acuna, S., and Teh, S.J. (2015) Contaminant and food limitation stress in an endangered estuarine fish. *Sci Tot Environ* **532:** 316–326.

Hansen, P.J. (2002) Effect of pH on growth and survival of marine phytoplankton: implications for species succession. *Aquat Microb Ecol* **28:** 279–288.

Hestir, E.L. (2010) Trends in estuarine water quality and submerged aquatic vegetation. Doctoral dissertation. Davis: University of California-Davis.

Hobbs, J.A., Bennett, W.A., and Burton, J.E. (2006) Assessing nursery habitat quality for native smelts (Osmeridae) in the low-salinity zone of the San Francsico estuary. *J Fish Biol* **609:** 907–922.

Horner-Devine, M.C., Leibold, M.A., Smith, V.H., and Bohannan, B.J.M. (2003) Bacterial diversity patterns along a gradient of primary productivity. *Ecol Lett* **6:** 613–622.

Huisman, J., Sharples, J., Stroom, J.M., Visser, P.M., Kardinaal, W.E.A., and Sommeijer, J. (2004) Changes in turbulent mixing shift competition for light between phytoplankton species. *Ecology* **85:** 2960–2970.

Humbert, J.F., Barbe, V., Latifi, A., Gugger, M., Calteau, A., Coursin, T., *et al*. (2013) A tribute to disorder in the genome of the bloom-forming freshwater cyanobacterium *Microcystis aeruginosa*. *PLoS One* **8:** e70747.

Huson, D.H., Mitra, S., Weber, N., Ruscheweyh, H., and Schuster, S.C. (2011) Integrative analysis of environmental sequences using MEGAN4. *Genome Res* **21:** 1552–1560.

Janse, I., Meima, M., Kardinaal, W.E.A., and Zwart, G. (2003) High-resolution differentiation of cyanobacteria by using rRNA-internal transcribed spacer denaturing gradient gel electrophoresis. *Appl Environ Microbiol* **69:** 6634–6643.

Jassby, A.D., (2008). Phytoplankton in the upper San Francisco Estuary: Recent biomass trends, their causes, and their trophic significance. *San Francisco Estuary and Watershed Science* **6:** 2.

Jones, G.J., Bourne, D.G., Blakeley, R.L., and Doelle, H. (1994) Degradation of the cyanobacterial hepatotoxin microcystins by aquatic bacteria. *Nat Toxins* **2:** 228–235.

Kehr, J.C., Gatte, P.D., and Dittmann, E. (2011) Natural product biosyntheses in cyanobacteria: a treasure trove of unique enzymes. *Beilstein J Org Chem* **7:** 1622–1635.

Kimmerer, W. (2005) Long-term changes in apparent uptake of silica in the San Francisco estuary. *Limnol Oceanogr* **50:** 793–798.

Klein Breteler, W.C.M., Schogt, N., Baas, M., Schouten, S., and Kraay, G.W. (1999) Trophic upgrading of food quality by protozoans enhancing copepod growth: role of essential lipids. *Mar Biol* **135:** 191–198.

Komoroske, L.M., Connon, R.E., Lindberg, J., Cheng, B.S., Castillo, G., Hasenbein, M., and Fangue, N.A. (2014) Ontogeny influences sensitivity to climate change stressors in an endangered fish. *Conserv Physiol* **2:** cou008.

Krevš, A., Koreivienė, J., and Mažeikaitė, S. (2010) Plankton food web structure during cyanobacteria bloom in the highly eutrophic Lake Gineitiškės. *Ekologija* **56:** 47–54.

Kurmayer, R., and Kutzenberger, T. (2003) Application of real-time PCR for quantification of microcystin genotypes in a population of the toxic cyanobacterium *Microcystis* sp. *Appl Environ Microbiol* **69:** 6723–6730.

Lampert, W. (1987) Laboratory studies on zooplankton-cyanobacteria interactions. *NZ J Mar Freshwater Res* **21:** 483–490.

Leflaive, J.P., and Ten-Hage, L. (2007) Algal and cyanobacterial secondary metabolites in freshwaters: a comparison of allelopathic compounds and toxins. *Freshwater Biol* **52:** 199–214.

Legrand, C., Rengefors, K., Fistarol, G.O., and Granéli, E. (2003) Allelopathy in phytoplankton – biochemical, ecological and evolutionary aspects. *Phycologia* **42:** 406–419.

Lehman, P.W., Boyer, G., Satchwell, M., and Waller, S. (2008) The influence of environmental conditions on the seasonal variation of *Microcystis* cell density and microcystins concentration in San Francisco Estuary. *Hydrobiologia* **600:** 187–204.

Lehman, P.W., Teh, S.J., Boyer, G.L., Nobriga, M.L., Bass, E., and Hogle, C. (2010) Initial impacts of *Microcystis aeruginosa* blooms on the aquatic food web in the San Francisco Estuary. *Hydrobiologia* **637:** 229–248.

Lehman, P.W., Marr, K., Boyer, G.L., Acuna, S., and Teh, S.J. (2013) Long-term trends and causal factors associated with *Microcystis* abundance and toxicity in San Francisco Estuary and implications for climate change impacts. *Hydrobiologia* **718:** 141–158.

Leikoski, N., Fewer, D.P., Jokela, J., Alakoski, P., Wahlsten, M., and Sivonen, K. (2012) Analysis of an inactive cyanobactin biosynthetic gene cluster leads to discovery of new natural products from strains of the genus *Microcystis*. *PLoS One* **7:** e43002.

Li, H., and Durbin, R. (2009) Fast and accurate short read alignment with Burrows-Wheeler transform. *Bioinformatics* **25:** 1754–1760.

Li, H., Handsaker, B., Wysoker, A., Fennell, T., Ruan, J., Homer, N., *et al*. (2009). The Sequence Alignment/Map format and SAMtools. *Bioinformatics* **25:** 2078–2079.

Liu, S., Ren, H., Shen, L., Lou, L., Tian, G., Zheng, P., and Hu, B. (2015) pH levels drive bacterial community structure in sediments of the Qiantang River as determined by 454 pyrosequencing. *Front Microbiol* **6:** 285.

Louati, I., Pascault, N., Debroas, D., Bernard, C., Humbert, F.F., and Leloup, J. (2015) Structural Diversity of Bacterial Communities Associated with Bloom-Forming Freshwater Cyanobacteria Differs According to the Cyanobacterial Genus. *PLOS ONE* **10:** e0140614.

Lucas, L.V., and Thompson, J.K. (2012) Changing restoration rules: exotic bivalves interact with residence time and depth to control phytoplankton productivity. *Ecosphere* **3:** 1–26.

Malbrouck, C., and Kestemont, P. (2006) Effects of microcystins on fish. *Environ Toxicol Chem* **25:** 72–86.

Martinez-Garcia, M., Brazel, D.M., Swan, B.K., Arnosti, C., Chain, P.S.G., Reitenga, K.G., *et al.* (2012) Capturing single cell genomes of active polysaccharide degraders: an unexpected contribution of *Verrucomicrobia*. *PLoS One* **7:** e35314.

Mikalsen, B., Boison, G., Skulberg, O.M., Fastner, J., Davies, W., Gabrielsen, T.M., *et al.* (2003) Natural variation in the microcystin synthetase operon *mcyabc* and impact on microcystin production in *Microcystis* strains. *J Bacteriol* **185:** 2774–2785.

Moisander, P.H., Lehman, P.W., Ochiai, M., and Corum, S. (2009) Diversity of *Microcystis aeruginosa* in the Klamath River and San Francisco Bay delta, California, USA. *Aquat Microb Ecol* **57:** 19–31.

Monsen, N.E., Cloern, J.E., Lucas, L.V., and Monismith, S.G. (2002) A comment on the use of flushing time, residence time, and age as transport time scales. *Limnol Oceanogr* **47:** 1545–1553.

Moustaka-Gouni, M., and Vardaka, E. (2006) Plankton food web structure in a eutrophic polymictic lake with a history of toxic cyanobacterial blooms. *Limnol Oceanogr* **51:** 715–727.

Nichols, F.H., Thompson, J.K., and Shemel, L.E. (1990) Remarkable invasion of San-Francisco Bay (California, USA) by the Asian clam *Potamocorbula amurensis*. 2. Displacement of a former community. *Mar Ecol Prog Ser* **66:** 95–101.

Nishizawa, A., Arshad, A.B., Nishizawa, T., Asayama, M., Fujii, K., Nakano, T., Harada, K., and Shirai, M. (2007) Cloning and characterization of a new hetero-gene cluster of nonribosomal peptide synthetase and polyketide synthase from the cyanobacterium *Microcystis aeruginosa* K-139. *J Gen Appl Microbiol* **53:** 17–27.

Nobriga, M.L., Feyrer, F., Baxter, R.D., and Chotkowski, M. (2005) Fish community ecology in an altered river delta: species composition, life history strategies and biomass. *Estuaries* **28:** 776–785.

Otten, T.G., and Paerl, H.W. (2011) Phylogenetic inference of colony isolates comprising seasonal *Microcystis* blooms in Lake Taihu, China. *Microb Ecol* **62:** 907–918.

Otten, T.G., and Paerl, H.W. (2015) Health effects of toxic cyanobacteria in U.S. Drinking and Recreational Waters: our current understanding and proposed direction. *Curr Environ Health Rpt* **2:** 75–84.

Otten, T.G., Xu, H., Qin, B., Zhu, G., and Paerl, H.W. (2012) Spatiotemporal patterns and ecophysiology of toxigenic *Microcystis* blooms in Lake Taihu, China: implications for water quality management. *Environ Sci Technol* **46:** 3480–3488.

Otten, T.G., Crosswell, J.R., Mackey, S., and Dreher, T.W. (2015) Application of molecular tools for microbial source tracking and public health assessment of a *Microcystis* bloom traversing 300km of the Klamath River. *Harmful Algae* **46:** 71–81.

Otten, T.G., Graham, J.L., Harris, T.D., and Dreher, T.W. (2016) Elucidation of taste-and odor-producing bacteria and toxigenic cyanobacteria in a midwestern drinking water supply reservoir by shotgun metagenomic analysis. *Appl Environ Microbiol* **82:** 5410–5420.

Ou, T., Gao, X.C., Li, S.H., and Zhang, Q.Y. (2015) Genome analysis and gene *nblA* identification of *Microcystis aeruginosa* myovirus (MaMV-DC) reveal the evidence for horizontal gene transfer events between cyanomyovirus and host. *J Gen Virol* **96:** 3681–3697.

Paerl, H.W., and Millie, D.F. (1996) Physiological ecology of toxic cyanobacteria. *Phycologia* **35:** 160–167.

Paerl, H.W., and Otten, T.G. (2013) Harmful cyanobacterial blooms: causes, consequences, and controls. *Microbial Ecol* **65:** 995–1010.

Paerl, H.W., and Otten, T.G. (2016) Duelling 'CyanoHABs': unravelling the environmental drivers controlling dominance and succession among diazotrophic and non-N_2-fixing harmful cyanobacteria. *Environ Microbiol* **18:** 316–324.

Park, H.D., Sasaki, Y., Maruyama, T., Yanagisawa, E., Hiraishi, A., and Kato, K. (2001) Degradation of the cyanobacterial hepatotoxin microcystin by a new bacterium isolated from hypertrophic lake. *Environ Toxicol* **16:** 337–343.

Parker, A.E., Dugdale, R.C., and Wilkerson, F.P. (2012) Elevated ammonium concentrations from wastewater discharge depress primary productivity in the Sacramento River and the Northern San Francisco Estuary. *Mar Poll Bull* **64:** 574–586.

Parveen, B., Ravet, V., Djediat, C., Mary, I., Quiblier, C., Debroas, D., and Humbert, J.F. (2013) Bacterial communities associated with *Microcystis* colonies differ from free-living communities living in the same ecosystem. *Environ Microbiol Rep* **5:** 716–724.

Penn, K., Wang, J., Fernando, S.C., and Thompson, J.R. (2014) Secondary metabolite gene expression and interplay of bacterial functions in a tropical freshwater cyanobacterial bloom. *ISME J* **8:** 1866–1878.

Peng, Y., Leung, H.C., Yiu, S.M., and Chin, F.Y. (2012) IDBA-UD: a de novo assembler for single-cell and metagenomic sequencing data with highly uneven depth. *Bioinformatics* **28:** 1420–1428.

Porter, K.G., Sherr, E.B., Sherr, B.F., Pace, M., and Sanders, R.W. (1985). Protozoa in planktonic food webs. *J Protozool* **32:** 409–415.

Puddick, J., Prinsep, M.R., Wood, S.A., Kaufononga, S.A.F., Cary, S.C., and Hamilton, D.P. (2014) High levels of structural diversity observed in microcystins from *Microcystis* CAWBG11 and characterization of six new microcystin congeners. *Mar Drugs* **12:** 5372–5395.

Rideout, J.R., He, Y., Navas-Molina, J.A., Walters, W.A., Ursell, L.K., Gibbons, S.M., *et al.* (2014) Subsampled open-reference clustering creates consistent, comprehensive OTU definitions and scales to billions of sequences. *Peer J* **2:** e545.

Rodriguez-R, L.M., and Konstantinidis, K.T. (2014) Nonpareil: a redundancy-based approach to assess the level of coverage in metagenomic datasets. *Bioinformatics* **30:** 629–635.

Rohrlack, T., Christoffersen, K., Kaebernick, M., and Neilan, B.A. (2004) Cyanobacterial protease inhibitor microviridin j causes a lethal molting disruption in *Dapnia pulicaria*. *Appl Environ Microbiol* **70:** 5047–5050.

Röttig, M., Medema, M.H., Blin, K., Weber, T., Rausch, C., and Kohlbacher, O. (2011) NRPSpredictor2–a web server for predicting NRPS adenylation domain specificity. *Nucleic Acids Res* **39:** W362–W367.

Sedmak, B., and Eleršek, T. (2005) Microcystins induce morphological and physiological changes in selected representative phytoplanktons. *Microbial Ecol* **50:** 298–305.

Segovia, B.T., Pereira, D.G., Bini, L.M., Ramos de Meira, B., Nishida, V.S., Lansac-Tôha, F.A., *et al.* (2015) The role of microorganisms in a planktonic food web of a floodplain lake. *Microb Ecol* **69:** 225–233.

Slater, S.B., and Baxter, R.D. (2014) Diet, prey selection, and body condition of age-0 delta smelt, Hypomesus transpacificus, in the Upper San Francisco Estuary. *San Francisco Estuary Watershed Sci* **12:** 1.

Smith, V.H. (1986) Light and nutrient effects on the relative biomass of blue-green algae in lake phytoplankton. *Can J Fish Aquat* **43:** 148–153.

Smith, G.D., and Doan, N.T. (1999) Cyanobacterial metabolites with bioactivity against photosynthesis in cyanobacteria, algae and higher plants. *J Appl Phycol* **11:** 337–344.

Sommer, T., Armor, C., Baxter, R., Breuer, R., Brown, L., Chotkowski, M., *et al.* (2007) The collapse of pelagic fishes in the Upper San Francisco Estuary. *Fisheries* **32:** 270–277.

Søndergaard, M., Riemann, B., and Jørgensen, N.O.G. (1985) Extracellular organic carbon (EOC) released by phytoplankton and bacterial production. *Oikos* **45:** 323–332.

Spietz, R.L., Williams, C.M., Rocap, G., and Horner-Devine, M.C. (2015) A dissolved oxygen threshold for shifts in bacterial community structure in a seasonally hypoxic estuary. *PLoS One* **10:** e0135731.

Stachelhaus, T., Mootz, H.D., and Marahiel, M.A. (1999) The specificity-conferring code of adenylation domains in nonribosomal peptide synthetases. *Chem Biol* **6:** 493–505.

Steffen, M.M., Li, Z., Effler, T.C., Hauser, L.J., Boyer, G.L., and Wilhelm, S.W. (2012) Comparative metagenomics of toxic freshwater cyanobacteria bloom communities on two continents. *PLoS One* **7:** e44002.

Thomson, J.R., Kimmerer, W.J., Brown, L.R., Newman, K.B., Mac Nally, R., Bennett, W.A., Feyrer, F., and Fleishman, E. (2010) Bayesian change point analysis of abundance trends for pelagic fishes in the upper San Francsico Estuary. *Ecol Appl* **20:** 1431–1448.

Tillett, D., Dittmann, E., Erhard, M., von Döhren, H., Börner, T., and Neilan, B.A. (2000) Structural organization of microcystin biosynthesis in *Microcystis aeruginosa* PCC7806: an integrated peptide-polyketide synthetase system. *Chem Biol* **7:** 753–764.

Van Hannen, E.J., Zwart, G., van Agterveld, M.P., Gons, H.J., Ebert, J., and Laanbroek, H.J. (1999) Changes in bacterial and eukaryotic community structure after mass lysis of filamentous cyanobacteria associated with viruses. *Appl Environ Microbiol* **65:** 795–801.

Von Elert, E., and Wolffrom, T. (2001) Supplementation of cyanobacterial food with polyunsaturated fatty acids does not improve growth of *Daphnia*. *Limnol Oceanogr* **46:** 1552–1558.

Von Elert, E., Martin-Creuzburg, D.M., and LeCoz, J.R. (2003) Absence of sterols constrains carbon transfer between cyanobacteria and freshwater herbivore (*Daphnia galeata*). *Proc R Soc Lond Ser B Biol Sci* **270:** 1209–1214.

Von Elert, E., Agrawal, M.K., Gebauer, C., Jaensch, H., Bauer, U., and Zitt, A. (2004) Protease activity in gut of *Daphnia magna*: evidence for trypsin and chymotrypsin enzymes. *Comp Biochem Physiol B* **137:** 287–296.

Welker, M., and von Döhren, H. (2006) Cyanobacterial peptides - Nature's own combinatorial biosynthesis. *FEMS Microbiol Rev* **30:** 530–563.

Wiegand, C., and Pflugmacher, S. (2005) Ecotoxicological effects of selected cyanobacterial metabolites a short review. *Toxicol Appl Pharmacol* **203:** 201–218.

Williams, R.J., Howe, A., and Hofmockel, K.S. (2014) Demonstrating microbial co-occurrence pattern analyses within and between ecosystems. *Front Microbiol* **5:** 358.

Wilson, A.E., Sarnelle, O., and Tillmanns, A.R. (2006) Effects of cyanobacterial toxicity and morphology on the population growth of freshwater zooplankton: meta-analyses of laboratory experiments. *Limnol Oceanogr* **51:** 1915–1924.

Woodhouse, J.N., Kinsela, A.S., Collins, R.N., Bowling, L.C., Honeyman, G.L., Holliday, J.K., and Neilan, B.A. (2016) Microbial communities reflect temporal changes in cyanobacterial composition in a shallow ephemeral freshwater lake. *ISME J* **10:** 1337–1351.

Ye, Y., Choi, J.H., and Tang, H. (2011) RAPSearch: a fast protein similarity search tool for short reads. *BMC Bioinform* **12:** 159.

York, J.K., McManus, G.B., Kimmerer, W.J., Slaughter, A.M., and Ignoffo, T.R. (2014) Trophic links in the plankton in the low salinity zone of a large temperate estuary: top-down effects of introduced copepods. *Estuar Coasts* **37:** 576–588.

Yoshida, T., Nagasaki, K., Takashima, Y., Shirai, Y., Tomaru, Y., Takao, Y., *et al.* (2008) Ma-LMM01 infecting toxic *Microcystis aeruginosa* illuminates diverse cyanophage genome strategies. *J Bacteriol* **190:** 1762–1772.

Zeglin, L.H. (2015) Stream microbial diversity in response to environmental changes: review and synthesis of existing research. *Front Microbiol* **6:** 454.

Supporting information

Additional Supporting Information may be found in the online version of this article at the publisher's web-site:

Fig. S1. Map of study sites in the Delta region of the San Francisco Estuary: ANT = Antioch, FRK = Franks Tract, MIL = Mildred island, MOK = Mokelumne River, OLD = Old River, RIO = Rio Vista (Sacramento River).

Fig. S2. (A) *Microcystis* sp. bloom at Mildred Island (27-Aug, 2012); (B) *Microcystis* 'flake' colonial morphology at 40× and 400× magnification; (C) *Microcystis* 'torn' colonial morphology at 40× and 400× magnification; (D)

Microcystis 'web' colonial morphology at 40× and 400× magnification.

Fig. S3. Bayesian inference of *Microcystis* phylogenies utilizing 16S-23S rRNA ITS clone libraries from Delta *Microcystis* sp. colony isolates and 454 deep sequencing (OTUs) aligned using a GTR model with gamma distributed rate variation; bootstrap values are indicated at the nodes and the scale bar represents changes per nucleotide.

Fig. S4. Amino acid profile of *mcyB*1 adenylation domains from Sanger sequenced colony isolates. Conserved substitutions indicate the presence of at least six different microcystin-producing *Microcystis* genotypes comprising the SFE population. Analysis of adenylation domain amino acid binding pockets, denoted by asterisks (*) along the top of the alignments, predicted that genotypes I, II, III, V and VI produce MC-RR and genotype IV produces MC-LR.

Fig. S5. *Microcystis* cell counts conducted on 2012 Mildred Island samples collected at 0.2 and 3 m depth.

Fig. S6. Network (co-occurrence) analysis of 16S rRNA amplicon OTUs, only strongly significant ($p < 0.05$) interactions are displayed; (A) positive interactions ($r > 0.75$); and (B) negative interactions ($r < -0.75$); in both figures *Microcystis* is highlighted in red.

Fig. S7. PCR screening for *Microcystis* secondary metabolites (aeruginosin, cyanopeptolin, micropeptin, microviridin and piricyclamide) in the peak-*Microcystis* bloom sample collected at Mildred Island (27 Aug, 2012), a microcystin-negative *Microcystis aeruginosa* culture (UTEX2386) and a microcystin-positive *Microcystis aeruginosa* culture (UTEX2667).

Table S1. Primers and probes used in study and their thermal cycling conditions.

Table S2. Breakdown of cyanobacterial community based on 454 pyrosequencing of cyanobacteria-specific 16S-23S rRNA ITS amplicons.

Table S3. Stacklehaus codes for McyB1 and McyC1 amino acid adenylation domains observed in the Delta *Microcystis* population. The Groups refer to the colony PCR sequences and the contigs refer to the metagenome assembly.

Table S4. Identification of contigs from putative *Microcystis* cyanophage with high nucleotide similarity to two closely related *Microcystis* cyanophage genomes and their relative read coverage depth for three Mildred Island samples collected in 2012.